



National University of Lesotho



**Investigating viability of using solar thermal energy for optimizing
the gas yields for biogas in Lesotho**

TABEMPE EDGAR LESENYEHO

200100507

A dissertation submitted in partial fulfilment of
the requirements for the degree of

Master of Science in Sustainable Energy

Offered by the

Energy Research Centre

Faculty of Science & Technology

APRIL 2021

Table of Contents

List of figures.....	ii
List of tables	iv
Abstract.....	iv
Acknowledgments	vii
Dedication	viii
1.0 Introduction.....	1
1.1 Background.....	1
1.2 Theoretical framework.....	4
1.3 Research questions.....	6
1.4 Research objectives.....	6
1.5 Dissertation organization.....	7
2.0 Literature review	8
2.1 How biogas works.....	8
2.2 Studies conducted on the enhancement of biogas production	10
2.3 Solar thermal and how it works	12
2.4 Solar radiation data.....	14
2.5 Different models used for predicting solar radiation on a tilted surface	15
2.6 Equations of the thermal model.....	20
2.7 Factors affecting the performance of the solar thermal collector.....	23
2.7.1 Collector efficiency	23
2.7.2 Incident angle modifier	25
2.8 Heat exchanger theory and capacity factor	26
2.9.1 Temperature in a storage tank.....	28
2.9.3 Economic and thermal analysis	31
2.9.4 Collector selection criteria	31
2.9.4.1 Net Present Value calculation.....	32
2.9.4.3 Internal Rate of Return	33
2.9.4.4 Payback Period	33
2.9.4.5 Levelized Cost of Energy	34
2.9.4.6 Benefit-Cost Ratio.....	35
2.9.5 Literature synthesis.....	35
3.0 Materials and Methods.....	38
3.1 Microsoft excel model.....	39

3.2 Solar radiation inputs and assumptions.....	40
3.3 Determination of solar radiation on a tilted surface.....	40
3.4 Other system inputs.....	41
3.5 Description of the model used for integration of solar thermal into biogas.....	42
3.6 Energy balance of solar water storage.....	43
3.7 Energy balance of the digester.....	45
3.8 Sizing the solar thermal storage.....	47
3.9 Collector selection criterion	50
4.0 Results and discussions.....	55
4.1 Economic analysis of the system	71
4.1.1 Cash flow analysis.....	71
4.1.2 System optimization	71
4.1.3 Project Pay back Period.....	75
4.1.4 Net Present Value	76
4.1.4 Internal Rate of Return.....	77
4.1.5 Validation of results.....	78
4.1.6 Limitations of the study	79
5.0. Conclusion and recommendations.....	80
6.0 References.....	82

List of figures

Figure 1: Effects of increasing the temperature on the volume of biogas yield[9]	4
Figure 2: Optimally sized system [10]	5
Figure 3: Schematic layout of solar-anaerobic digester [11]	6

Figure 4: Classification of anaerobic digester for various parameters[14]	10
Figure 5: Domestic solar water heating system model[10]	14
Figure 6 : Zenith angle, slope, surface azimuth, and solar azimuth angle [34]	20
Figure 7: Collector efficiency against $(T_{in}-T_a)/G$ [10]	25
Figure 8: Variation of $K\tau\alpha$ with $1/\cos\theta - 1$ for flat plate and evacuated tube collector [10]	27
Figure 9: Schematic of a liquid system with a collector heat exchanger between collector and storage tank[28]	28
Figure 10: Heat exchanger correction factor function of mC_{pmin}/mC_{pc} and $mC_p/ACFRUL$ [30]	29
Figure 11: Proposed schematic for solar integrated bio digester system.....	43
Figure 12: Digester temperature against the volume of biogas produced	47
Figure 13: Collector area, storage surface, and storage volume	49
Figure 14: Coefficients for Evacuated Tube collector	52
Figure 15: Coefficients for Flate Plate collector	52
Figure 16: Variation of the angle of incidence beam radiation and reflected radiation .	57
Figure 17 :Variation of radiation on a tilted surface and collector energy output	58
Figure 18: Variation of collector energy and efficiency over a day	59
Figure 19: System temperatures	60
Figure 20: Volume of biogas without solar thermal energy and with solar thermal energy	63
Figure 21: Percentage and volume of biogas produced at different collector areas	68
Figure 22: : Payback Period	72
Figure 23: Collector area against Net Present Value	73
Figure 24: Internal Rate of Return	74

tables

Table 1: Relationship between angle of incident of beam and incident angle modifier .
51
Table 2: Solar thermal collector ranking using energy per dollar criterion
56 Table 3: Variation of collector area, the volume of biogas produced and greenhouse
gas
averted
64 Table 4: Cash flow analysis for the project lifetime
..... 71
Table 5:Results for economic assessment of an integrated solar assisted solar biogas 75

Abstract

Selection of the solar thermal collector using the energy per dollar matrix, prevailing interest rate and the prevailing inflation rate is of paramount importance for decision-making for investment in solar-assisted biodigesters. This paper presents a comprehensive computer-based excel model on investigating the viability of using solar thermal energy for optimizing the biogas yields in Lesotho. The excel based model is used to analyze both the thermal and economic performance of the solar-assisted biogas digester. The model determines solar thermal performance, solar thermal collector size, solar storage size, as well as the surface area over which the heat losses occur in both the solar water heater and biodigester tank. It will further look into economic analysis of the system.

In order to ensure maximum benefits, sizing of the solar thermal system has been carried out to give the optimum solution. Simulations have been performed on an hourly time step. Comparison of production of biogas with solar thermal energy and production of biogas without solar thermal energy were undertaken to find the effects of temperature on the production of biogas. It was found that the production of biogas is optimum at the mesophilic temperatures of 18⁰ C to 30⁰ C.

Different collectors, both evacuated tube collectors and flat plate collectors which are valued by Solar Ratings & Certificate Corporation are ranked using energy per dollar matrix. The Sun power evacuated tube collector is the best collector used for system design since it has high energy per dollar of 25.3 kWh and low heat loss parameters. The Net Present Value is the objective function to optimize for the solar thermal system.

The optimum collector area to deploy for 5 m^3 biodigester is 16 m^2 , the optimum solar storage tank of 800 liters is required. The total cost of buying the collector and the solar storage tank is \$1744. In Lesotho 1 m^3 of biodigester requires a solar thermal collector area of about 3 m^2 . The optimum collector area gives a maximum Net Present Value of \$1854. Moreover, the biogas produced is 396 m^3 per annum with the percentage increase of extra biogas as 11.5% per annum. The project is economically viable with a Net Present Value of \$1854, an Internal Rate of Return of 10.36%, a Payback period of 9 years, and a Benefit-Cost Ratio of 2.01. The project lifetime is 20 years.

Keywords: *marginal diminishing returns, energy per dollar matrix, solar thermal energy, optimum collector area, economic performance indicators*

Nomenclature

DWHS	Domestic water heating systems
SE4ALL	Sustainable energy for all
UASB	Up-flow anaerobic sludge blanket
TRNSYS	The transient systems simulation program
TMY	Typical Meteorological Year
NSRDB	National Solar Radiation Database
G	Solar irradiance
T_a	Air ambient temperature
$\tau\alpha$	Transmittance-absorption product
IAM	Incident angle modifier
F_R	Heat removal factor
F_{RUL}	Heat loss parameter
$F_{R\tau\alpha}$	Collector efficiency
Δt	Finite-time –step period over which the solar thermal process is simulated
T_s	The temperature of hot water storage contents at the beginning of period Δt [$^{\circ}\text{C}$]
ΔT_s	Temperature gain/loss for the storage tank during time –step period Δt [$^{\circ}\text{C}$]
T_{s+}	The temperature of storage tank contents at the end of Δt [$^{\circ}\text{C}$]
S_l	Storage losses

T_a	Ambient temperature [°C]
T_{load}	The temperature required by load [°C]
T_d	Digester temperature
T_{mains}	Incoming cold water temperature [°C]
Q_{coll}	Collector output energy
Q_u	Digester energy
NGOs	Non–Governmental Organizations
TED	Technologies for Economic
NPV	Development
IRR	Net Present Value
TMY	Internal Rate of Return
m_s	Typical meteorological year
ε_x	Digester mass flow rate Heat exchanger effectiveness
r	Discount rate
i	Interest rate
j	Inflation rate
OM	Operation and maintenance
E_{pd}	Energy per dollar
B_{ws}	Biogas without solar thermal energy
B_s	Biogas with solar thermal energy

Acknowledgments

I wish to express my sincere gratitude to my Supervisor Engineer Tawanda Hove for providing his time and support to guide me in the MSc dissertation, I feel honored. It was very difficult in the beginning, but you offered guidance and courage until I got back on track. Your support is highly valued.

Special thanks to ERC members for constructive criticism, support, motivation, and guidance through the entire MSc research. Your knowledge and high level of expertise has made it easy to go ahead with the research work. Special thanks to Ms. Mantopi Lebofa director of Technology for Economic Development (TED) for providing useful information about the biogas technology, in particular the price of the biogas. The management of Lesotho-China Fellowship Collegiate for providing time to study, and other members of the academic staff in particular Dr. Sepiriti Sepiriti and Mr. Meshack Foloko for moral support. Finally family members, brothers, and sisters who were prepared to motivate me whenever possible.

Dedication

I dedicate this work to my wife 'Makarabo Lesenyeho for providing unconditional support, courage and always being there for me. My late daughter Karabo Lesenyeho, who lost her life during my period of study, may her soul rest in peace.

1.0 Introduction

1.1 Background

In Lesotho, solar thermal technology has been widely used particularly for domestic heating systems (DWHS)[1]. An important point in solar thermal design is to determine the thermal output. It is also important to know the availability of solar radiation, collector tilt angle, and collector efficiency [1].

Solar thermal is the technology that converts the energy from the sun to produce heat for domestic hot water systems, space heating, and the production of electricity. Biogas is a gas resulting from the decomposition of organic matter into combustible gases such as hydrogen and methane and non-combustible gases such as carbon dioxide and hydrogen sulfide [2].

Several factors affect the production of biogas. Some of these factors are PH, moisture content, salinity, type of feedstock, and temperature. Temperature contributes most to biogas production. The organic matter is made up of carbon and nitrogen, Nitrogen increases the alkalinity of the digester content while carbon contributes to the acidic conditions of the digester's content.

Biogas requires a certain temperature for its optimum production. The temperature might not be favourable in the natural environment. The optimum temperatures are not always favourable, for example, thermophilic production requires temperatures from 45^o C up to 65^o C [3].The climate in Lesotho is not conducive ,since it is very cold in winter. The temperatures vary from -7^oC in winter months of the year to 32^oC in summer months of the year[1]. There is a need to make temperatures suitable so that the optimum heat can be obtained.

There are several ways to make temperatures favourable. It is proposed that one way of producing the optimum temperatures is by using solar thermal energy which is readily available, environmentally friendly, and free [4]. Solar thermal

energy could be the potential source of heat. It is renewable energy and does not require a source of fuel. Also, the sun is perpetual. That is the solar thermal energy will always be available since the sun will always rise. In Lesotho, the average clearness index is 0.61 and the number of daylight hours is 12 hours[1].Therefore the average number of sunshine hours is 12 hours multiplied by 365 days and average clearness index of 0.61.This about 3000 sunshine hours per year.This averages to about 8.5 sunshine hours per day.

The study investigates the viability of integrating solar thermal energy for optimizing the biogas yields for biogas plants in Lesotho. In Lesotho, it is extremely cold in winter. The cold temperatures affect the production of biogas plants. It is supposed that the problem could be solved by the integration of solar thermal energy into the existing biogas plant. Previous research has been focusing on the design of solar thermal technology and biogas technology systems as separate systems. The common problem is that the production of biogas decreases in winter due to low temperatures. However, it is supposed that introducing the new method of integrating solar thermal technology into biogas systems will enhance the production of biogas yield in Lesotho.

Furthermore, Lesotho is rich in solar resources with the average global solar radiation ranging from 15 MJ/m² to 20MJ/m² [5]. The results support the fact that indeed, Lesotho has the potential in solar resources which can be used for both photovoltaic systems and solar thermal systems.

One of the aims of nationally determined contributions and sustainable development goals is to ensure access to clean and affordable energy for all (SE4ALL). Both solar thermal and biogas play an important role in ensuring access to clean affordable energy. Waste is a resource that is always available, it is used as a bio-energy resource to maintain personal health, community health and to produce biofuels to increase access to energy.

The integration of solar thermal technology in biogas technology has been a topic of interest in research in different parts of the world. Similar studies have been done in Asia, Europe, and Africa. In Asia, the research reveals that the low temperatures result in low production of the biogas yield [6]. It was found that solar thermal energy is the potential source of energy to stabilize the temperature for optimum production of biogas. The previous literature indicated that using integrated solar thermal energy to achieve optimum temperatures for biogas production is sustainable through most of the years.

Another study similar to the one in Asia has been carried out in India. The study reveals that when co-digestion of different feedstock was subjected to different temperatures various biogas yields were obtained. It also emerged that the production of biogas depends on temperature. In sub-Saharan countries, a similar study was conducted in Ghana. It discovered that solar energy is needed to maintain the mesophilic condition of the biodigester. The results indicated that solar thermal energy is needed to maintain the temperatures to enhance the effectiveness of biogas production [7].

A lot of research has been done on investigating the viability of using solar thermal energy for biogas production; however, no such study has been conducted in Lesotho. As mentioned earlier in this section, the temperatures are low and this affects the production of biogas. The previous researches found out that the volume of the biogas produced increases with temperature, although the relationship is not linear [8]. The marginal product of biogas production is not a linear function. Therefore, there should be an optimum size of the heat source. There should be an optimum size of collector, solar storage tank size to deploy in order to determine the economic analysis of solar-assisted biodigester.

1.2 Theoretical framework

Previous research has found that an increase in the temperature results in a marginal increase in the volume of biogas yield. The graph of biogas produced against the temperature is not a linear function. This kind of variation means that there could be an optimum temperature where the maximum biogas yield is obtained. Figure 1 shows the effect of increasing the temperature on the volume of biogas yield. From the figure, it can be seen that for every increase in temperature there is a marginal increase in the production of biogas.

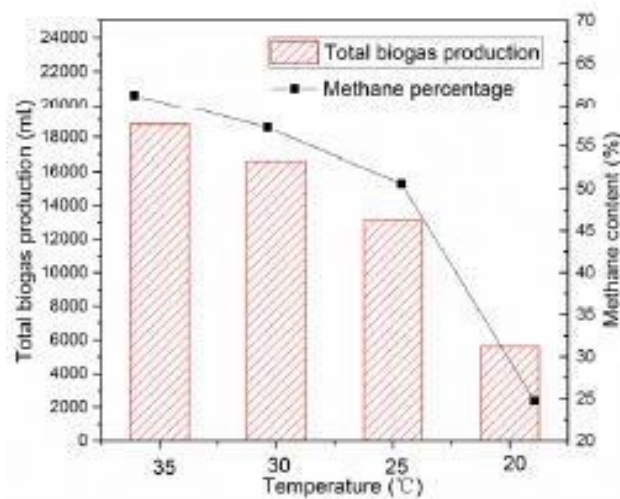


Figure 1: Effects of increasing the temperature on the volume of biogas yield[9]

Similarly, figure 2 shows the Net Present Value of solar savings, solar fraction against the collector area. There is a marginal increase in the heat output when

the collector is varied. There is an optimum collector area that gives the optimum temperature for the design.

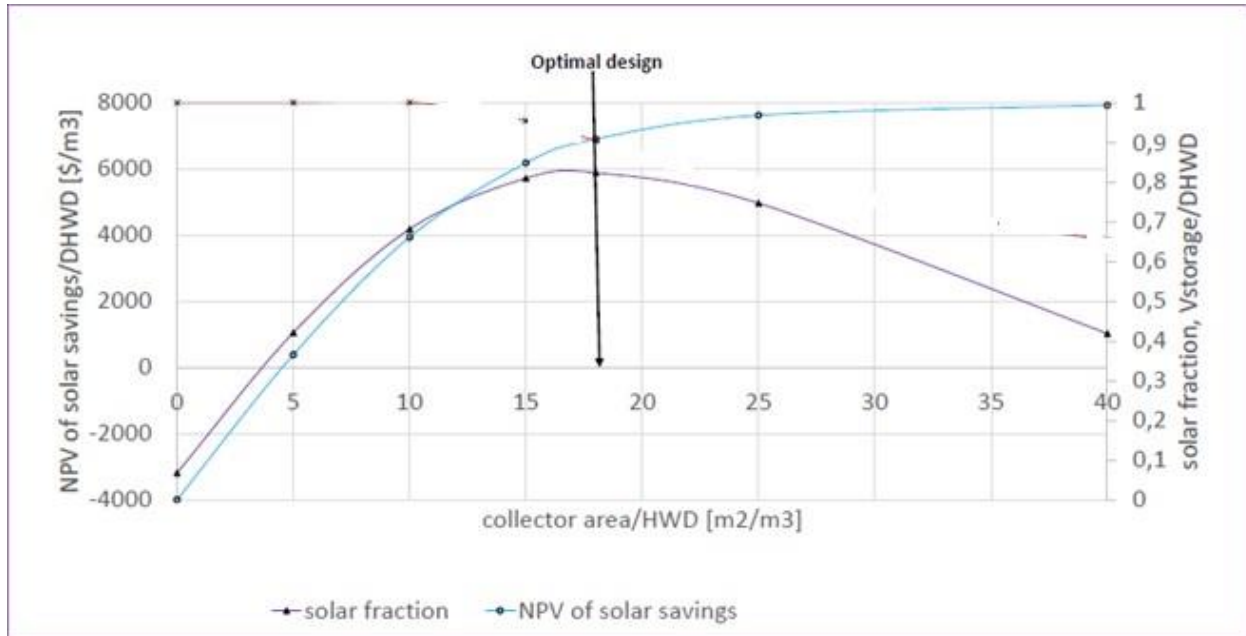


Figure 2: Optimally sized system [10]

In this case, solar thermal technology will be used to give optimum temperatures for instance 35°C. Putting too many collectors increases the cost of the collector. It is important to know the optimum collector area needed to install. [10]. Solar collectors are economic only beyond a certain solar fraction. This is going to limit the sizing of the solar thermal system.

When the collector area is varied, the Net Present Value (NPV) increases and temperature also increases. As the collector area is varied more, there will be a marginal increase in the temperature and volume of biogas produced. The task is to determine the sweet spot. The optimum collector area and the temperature are the two important factors that will be important for decision-making. If the NPV is positive then the project is viable and can be considered for implementation.

One way of doing this is to integrate the solar thermal collector outside the storage tank as illustrated in figure 3 so that the collector energy output is the one that goes inside the storage tank. The output of the collector is the one that heats the contents of the digester. How heat is transferred depends on temperature, the collector area, and the mass of the liquid.

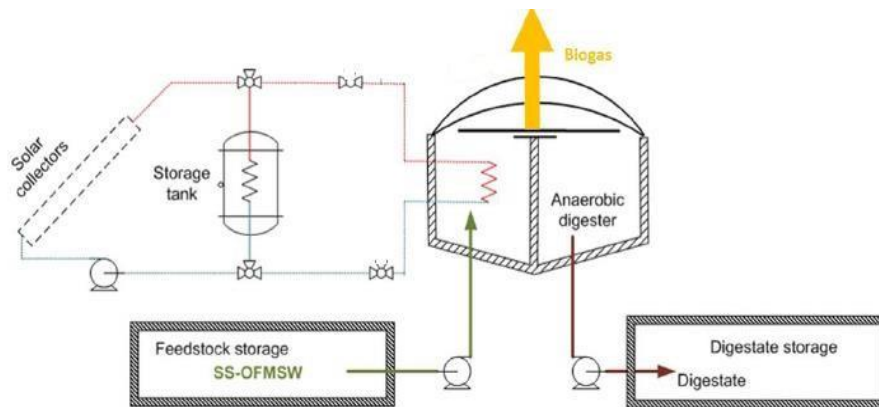


Figure 3: Schematic layout of solar-anaerobic digester [11]

1.3 Research questions

The study seeks to answer the following research questions.

- Is it economically viable to use solar thermal energy to enhance the effectiveness of biogas digestion?
- In order to maximize the economic viability, what is the extent of solar thermal energy deployment (for example number of solar collectors) in a biodigester system?

1.4 Research objectives

The main objective of the research is to investigate the technical and economic viability of using solar thermal energy for optimizing the gas yields for biogas

plants in Lesotho. To achieve this objective, the research objectives are broken into specific objectives as follows.

- To optimize the design of a system that uses solar thermal collectors to heat the contents of a biogas digester.
- To develop a computer model that can analyze the thermal performance of the collector-bio digester system as well as the economic performance of the system.
- To use the computer program to calculate the Net Present Values associated with each solar thermal collector size so that the system design can be economically optimized.

1.5 Dissertation organization

The dissertation is organized into five different sections. Section I is the introduction, which entails the study background, and the theoretical framework. It will further look into research questions and unpack the research objectives. Section II reviews the literature on investigating the viability of solar-assisted biogas digester in Lesotho. It will further look into the models that have been used in designing solar-assisted biogas digesters. Section III will be a methodology that includes data collection, economic viability, designing the computer-based model, and optimization of the results. Section IV will be the results and discussion while section V will be the conclusion and recommendations. Section VI will be the references.

In this chapter a general outline of the study objectives was given in line with my research objectives which is to investigate the technical and economic viability of using solar thermal energy for optimizing the gas yields for biogas plants in Lesotho.

In the next chapter the focus will be placed on literature review with regards to investigation of the economic viability using solar thermal energy for optimizing the gas yields for biogas in Lesotho.

2.0 Literature review

The discussed literature outlines research on the production of biogas and solar thermal and how they are affected by different temperatures. It also discusses biomass analysis, availability, conversion technologies, optimizing efficiency, and environmental impacts. As outlined in Hove 2018, solar thermal performances are discussed to find the economic viability of integrating solar collectors in the bio-digester.

2.1 How biogas works

Biogas results from biomass. It results from the decomposition of organic matter into combustible gases (Methane and hydrogen) and non-combustible gases (carbon dioxide and hydrogen sulfide). Biogas can be used for various applications such as heating, cooking, and combustion engines.

There are different methods used for the conversion of traditional biomass into modern biomass. The first one is a **thermochemical conversion** (combustion, gasification, liquefaction, and pyrolysis) which requires very high temperatures over 500°C[12]. Thermochemical conversion is used mainly in industrial applications. Combustion and gasification are used mainly to convert solid biomass into heat. Pyrolysis is used to convert biomass into biofuels. These conversion technologies are often expensive and produce large temperatures which are not suitable for biogas production because of the synthetic microbes which are sensitive to high temperatures.

The second one is **biochemical conversion** technologies (fermentation and anaerobic digestions) are used for the conversion of liquid biomass into ethanol and biogas respectively. According to [13], fermentation is used for commercial purposes to produce ethanol from sugar cane. Anaerobic digestion converts organic material directly into biogas through microorganisms. Compared to other conversion technologies, anaerobic digestion is most suitable in Lesotho because the country is rich in solar resources as outlined by the author in reference[1].

According to authors in reference [14], in their paper entitled a comprehensive review of the recent development and challenges of a solar-assisted biodigester system: it was found out that anaerobic digestion (AD) is the most effective process of producing biogas production. AD produces clean energy that has methane and carbon dioxide content. Methane content has a high energy content of 50 MJ/kg to 55MJ/kg that can be used mostly for industrial applications such as heating, production of electricity, and fuel [14].

Anaerobic digestion is the process of converting organic matter into biogas without the presence of oxygen [15]. The process of anaerobic digestion is affected by the physicochemical and biochemical properties of organic matter. There are four stages involved, hydrolysis, acidogenesis, acetogenesis, and methanogens [14]. Figure 4 shows a classification of anaerobic digestions for various parameters.

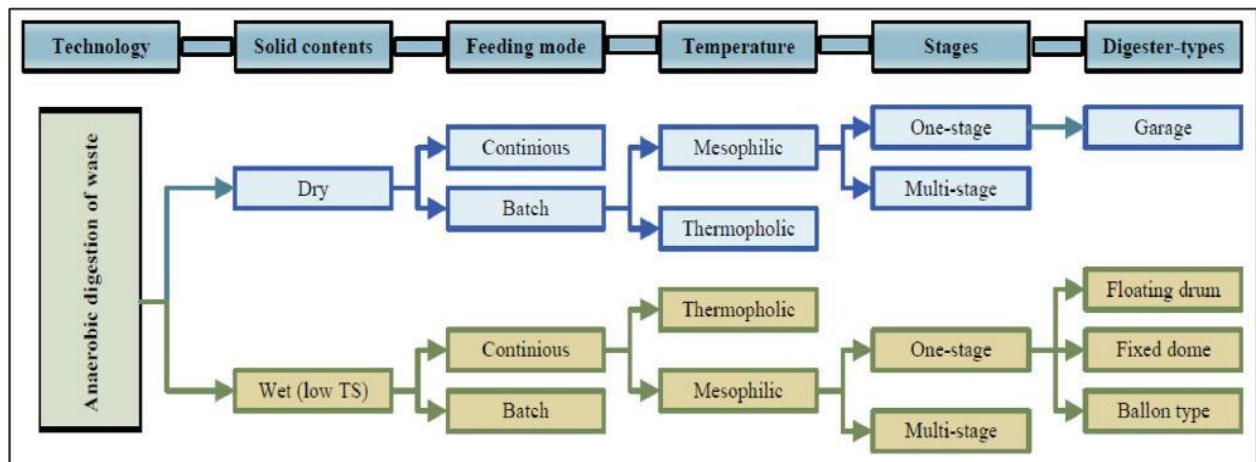


Figure 4: Classification of anaerobic digester for various parameters[14]

Several factors affect the production of biogas. These factors include PH, the salinity of water, type of feedstock, and temperature. The organic matter is made up of carbon and nitrogen, which increases the alkalinity of the digester content while carbon contributes to the acidic conditions of the digester's content. The author in reference [16] points out that the PH of the feedstock can greatly affect

the production of biogas. PH is the negative logarithm of hydrogen ions. Methane is produced in the PH range of 7.0 to 8.5 [16].

Although other parameters may interact, in this report other parameters are considered constant and optimized. One of the most important factors is temperature, assuming that all other factors are constant and optimized. There are about 80 biogas plants that are constructed by UNDP in Lesotho. However, 80 % of the biogas are no longer in operation [5]. It is suspected the cause might be due to the cold temperature in Lesotho. Temperatures vary from 32°C in summer to -7°C in winter [1]. There is a need to produce biogas in an optimum way using fewer resources.

There are many ways of increasing temperature. One way can be by heating biodigester, which also comes at a cost. One can do this by insulation and adding the heat source. Any heating can do. However, the heating that could do better is solar thermal energy because it is a renewable source of energy and it is abundant in Lesotho. Furthermore, the sun is free and there is no need to pay for it, but the problem is that it is intermittent [14].

2.2 Studies conducted on the enhancement of biogas production.

Several studies have been conducted in different parts of the world on investigating the viability of solar-assisted biogas production. A study was conducted by the author in reference [11] in Europe (Italy) on investigating the viability of solar-assisted biogas. It was concluded that solar thermal technology could reduce the amount of biogas used to heat the digester. Furthermore, it was concluded that solar thermal technology is economically viable if less expensive collectors are used. However, the study did not indicate for what volume of the digester and volume of the biogas gas yield was economically viable.

Another similar study conducted by the author in reference [6] in Asia in the rural areas of China. The two digesters were used, one fitted with a solar water heating system coupled with a heat exchanger and the other without the solar

water heating system. The results showed that the averages temperatures for the two digesters were 9.5 °C and 4.9 °C respectively above the ambient temperature with the biogas volume of 357 L/m³day 300m³/day [6]. Furthermore, it was concluded that solar thermal energy utilization produces sustainable biogas production in the rural areas of China.

Similarly, to the previous study the cost of solar water heating system plays a major role in the economic viability of the integrated solar thermal energy for optimization of biogas production. However, the volume of the biodigester was not mentioned as to which size of the digester biogas yields were obtained. The type of feedstock was kept constant on the two investigations.

In the United States of America, another study was investigated by the author in reference [17], to realize biological storage of solar thermal and solve the problems that solar energy system experienced which is the problem of intermittency. The research was an experimental investigation using manure digestion, co-digestion, and three different digesters of 10m³, 100m³, 1000 m³. It was found out that the solar storage efficiencies were 67%, 68% and 70% respectively.

Based on the foregoing, it was concluded that temperature is one of the most important factors that affect the production of biogas. Furthermore, it was concluded that the feedstock and other factors should be kept constant.

In Australia, a study conducted by the author in reference [14] showed that there several factors that affect biodigester efficiency, and the temperature is one of the most important factors. The temperature has a huge effect on mesophilic and thermophilic conditions. However, the research did not specify how much is the volume of the biogas produced and the size of the bio-digesters used. Moreover, the study did not reveal the temperature at which the volume of the biogas was achieved as well as the cost of the collector.

Another similar study to the previously discussed was carried out by the author in reference [18] in China, to improve the biogas production and maintain a constant temperature in winter using a $12m^3$ digester and insulation material.

The study revealed that a $12m^3$ bio-digester at $35^{\circ}C$ gave a biogas production rate of $0.63 m^3m^{-3} d^{-1}$.

Another similar study was conducted by the author in reference [19] in Africa (Morocco) using up-flow anaerobic sludge coupled with a solar thermal system. The system was simulated with the TRNSYS software. It was concluded that the solar heating systems and biodigesters produce 1.2 kW and 1.3 kW in winter and summer respectively [19]. Furthermore, it was concluded that the developed program allowed 100% saving of energy consumption.

In Lesotho, there is no study conducted on investigating the viability of solarassisted biogas for optimizing the gas yields hence the need to carry the study.

2.3 Solar thermal and how it works

Solar thermal is a technology that converts the sun's energy into heat. The solar thermal collector traps the radiation from the sun converts it into heat. The heat is transferred from the solar thermal collector to the solar storage tank. According to the author in reference [20], the heat transfer mechanism is based on the principle heat exchanger which transfers solar thermal energy through a special medium called anti-freeze or glycol. The medium transfers heat from the collector to the solar storage tank.

Figure 5 shows a solar water heater model for domestic water use. The system is a closed circulation system with a circulation pump, solar collectors, storage tank, and backup heater.

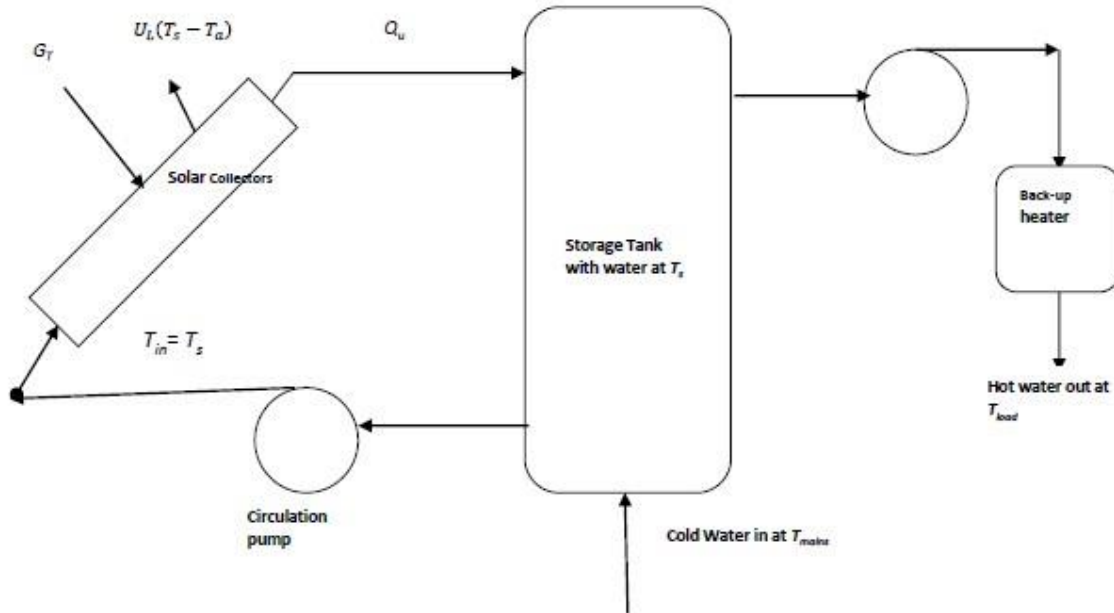


Figure 5: Domestic solar water heating system model[10]

Solar thermal collectors are classified into different categories such as design and working principle [20]. As outlined by the author in reference [21], solar thermal collectors can be classified into two categories, non-concentrating which is used for low-temperature applications and concentrating collectors which are used for high-temperature applications.

Concentrating collectors have a tracking mechanism to track the position of the sun. Concentrating collectors can achieve high temperatures more than nonconcentrating and are used widely in industrial applications.

Non-concentrating collectors are usually tilted at a latitude of the location. Nonconcentrating collectors have no tracking mechanism. A typical example is the flat plate collector. According to the author in reference [21], a flat plate collector consists of glazing covers, absorber plates, insulation layer, and tubes

filled with heat transfer fluid. The heat transfer fluid is responsible for transferring the liquid.

2.4 Solar radiation data

Solar radiation data tells us how much radiation is seen by the collector. Solar radiation data can be obtained from different forms such as ground data and satellite data. Ground data is not always available. On the other hand, satellite data is not accurate, because it is measured at the top of the atmosphere. It assumes extra-terrestrial radiation and measures the reflected radiation. Beam radiation can be found by inference between horizontal radiation and diffuse radiation. So, there is a need to develop atmospheric models to improve inferences.

The atmospheric models are different and the different values can be obtained. Most solar radiation data comes as monthly radiation which has to be converted into hourly radiation. The tilted plane models are used to predict the radiation on a tilted surface. In order to get fairly accurate data, satellite data has to be merged with ground measured data.

One way of obtaining solar radiation data is through Typical Meteorological Data (TMY) data. TMY data is mostly found in National Solar Radiation Database (NSRDB). TMY data contains one year of hourly data. TMY data is constructed by taking the monthly average which is on an hourly basis. For instance, TMY data selected from 2006 to 2016 might use averages for January 2010, averages for February 2009, averages for March 2011, and so on. It distributes radiation over a day on an hourly basis.

TMY data is typical since it condenses original solar radiation data and meteorological database for several years into just one year of data. TMY data has weather parameters such as ambient temperature, relative humidity, global horizontal radiation, beam radiation, diffuse radiation, wind speed, and surface pressure.

TMY data is found using latitude and longitude for a place over which study has to be considered. TMY data are available in System Advisor Models (SAM) and comma-separated values (CSV) format which is more user-friendly compared to TMY2 and TMY3 which were formerly used before development for the system advisor model. SAM model is free software that performs arduous system performance and predicts comprehensive financial cash flows of the system. CSV format files allow data to be stored in a format like a spreadsheet. TMY data are used mostly for computer simulation to predict estimates and performance of the solar systems at different locations[22],[23].

The solar radiation data is commonly available in the form of monthly daily radiation on a horizontal plane. It is important to know solar radiation on an hourly basis since the position of the sun on the sky concerning the surfaces varies hourly. The position of the sun is useful in energy calculations. It can also be used in various solar thermal applications.

2.5 Different models used for predicting solar radiation on a tilted surface.

There are several methods used to predict solar radiation on a tilted plane, to mention some but few, Temps-Coulson model, Klucher Model, Koronakis Model, Badsecu Model, Hay and Davis model, Reindl et.al Model, Muneer Model Perez et.al Model, HDKR (Hay, Klucher, Reindl) Model and Liu and Jordan Model [24],[25],[26]. These models have different complexity since they have too many variables that require a lot of data.

The Collares-Pereira and Rabl model has been used in several in some researches to determine radiation on a tilted surface[27],[26]. Collares-Pereira and Rabl model is the simplified Liu and Jordan model. It is an anisotropic model that assumes that the brightness of the sky is the same as the brightness of the surface. It considers the fact that the beam radiation comes from the general direction of the sun. It has a different concentration than the diffuse concentration coming from the earth.

Collares-Pereira sky model or diffuse model uses monthly averages data which are distributed over a day but not on an hourly basis. Collares-Pereira resolves daily monthly data into hourly data. The problem is that the hourly data is just diffuse, beam or total global radiation. The interest is on the radiation on a tilted surface. The models assume that the diffused radiation is distributed uniformly over the sky.

Collares-Pereira is simple and used in many applications as it does not require a lot of data. Different models need different data. Some need circumsolar radiation and anisotropic factors which are complex in terms of acquiring a lot of data [28]. Solar radiation data can be used to predict the performance of solar thermal collectors. Solar radiation data is available in different forms. The most detailed solar radiation data are beam radiation and diffuse radiation. Beam radiation is the radiation received by the earth without scattering while diffuse radiation is the radiation received by the earth after being intercepted by the atmosphere.

Available solar radiation data can be obtained from various sources. Some include meteorological stations and satellite data. However, there are problems associated with sources of data. The meteorological data obtained from the PVGIS is always 7% less than the National Aeronautics and Space Administration (NASA) [29]. Furthermore, meteorological data is not always available for different places while satellite data is also not always accurate. According to the author in reference [30], total solar radiation and diffuse radiation are measured on a horizontal surface. It is difficult to obtain beam radiation on a tilted surface. Beam radiation can be inferred as the difference between horizontal beam radiation and diffuse radiation. i.e.

$$I_b = I_h - I_d \quad (1)$$

Radiation on a tilted surface I_t is given by

$$I_t = I_B R_b + I_d \quad (2)$$

Where

I_t =radiation on the tilted surface

I_b =beam radiation

I_d =diffused radiation

R_b =reflected radiation

The reflected radiation R_b is given by equation 3

$$R_b = \frac{\cos \theta}{\cos \theta_z} \quad (3)$$

$\cos \theta$ Is given by equation 4

$$\begin{aligned} \cos \theta = & \sin \delta \sin \varphi \cos \beta + \sin \delta \cos \varphi \cos \gamma + \cos \delta \cos \varphi \cos \beta \cos \omega \\ & - \cos \delta \sin \varphi \sin \beta \cos \gamma \cos \omega \\ & + \cos \delta \sin \beta \sin \gamma \sin \omega \end{aligned} \quad (4)$$

or for a horizontal surface, the angle of incidence becomes the zenith angle and is given equation 5

$$\cos \theta = \cos \theta_z \cos \beta + \sin \theta_z \cos \beta \cos (\gamma_s - \gamma) \quad (5)$$

and

$$\cos \theta_z = \cos \varphi \cos \delta \cos \omega + \sin \varphi \sin \delta \quad (6)$$

$$\sin \theta_z = (1 - \cos \theta_z^2)^{1/2} \quad (7)$$

Where

θ =angle of incidence, the angle between beam radiation on surface and normal to the surface

θ_z =Zenith angle, the angle between the incidences of beam radiation on a horizontal surface.

Where

φ =latitude, the angular position north or south of the equator.

β =slope, the angle between the plane of the surface and the horizontal

N =average day number of the month on which the declination angle is calculated.

δ = declination angle.The declination δ , angle can be obtained by approximation using an equation of Copper(1969)[31],[32]. The declination angle ,depends on the day number(N), since the position of the sun varies over the day[33].

Illustrated in *equation 8* is an equation for the declination angle.

$$\delta = 23.45 \sin \left(\frac{360}{365} (N + 284) \right) \quad (8)$$

Another important angle that describes the position of the sun is the solar azimuth angle. It is an angular displacement from south of the projection of beam radiation on a horizontal plane[28]. Displacements east of the south are negative and west of the south are positive. Illustrated in *equation 9* is an equation for solar azimuth angle (γ_s).

$$\gamma_s = \text{sign}(\omega) \left| \cos^{-1} (\cos \theta_z \sin \varphi \cos \beta - \sin \delta) \right| \quad (9)$$

Parameters retain their meaning as in *equations 4*. Figure 5 shows the geometric relationship between a plane relative to the earth and the position of the sun relative to the plane.

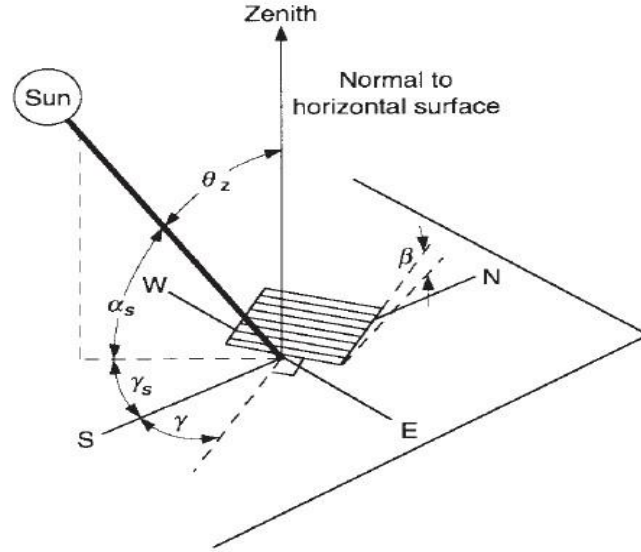


Figure 6 : Zenith angle, slope, surface azimuth, and solar azimuth angle [34]

R_b depends on the length of the day, time of the day, the tilt of the collector, whether the collector is facing the azimuth, and depends on the latitude. It is not the same through the year.

ω = hour angle, the angular displacement of the sun east or west of the local meridian. Hour angle is given by equation 10.

$$\omega = 15(t - 12) \quad (10)$$

Where t is solar time.

The sunset/sunrise hour angle (ω_s) on the horizontal surface occurs when $\theta_z = 90^\circ$ [33], $\cos\theta_z = 0$ and $\omega = \omega_s$, equation 6 simplifies to

$$\omega_s = \cos^{-1}(-\tan\phi\tan\delta) \quad (11)$$

The number of daylight hours (N_d) is given by equation 12.

$$N_d = \frac{2}{15} \omega_s = \frac{2}{15} \cos^{-1}(-\tan\phi\tan\delta) \quad (12)$$

2.6 Equations of the thermal model

The rate of useful energy extracted by collector (Q_{coll}) is equal to the rate of useful energy absorbed by a collector, less amount heat lost by a collector to its surroundings [10]. Depicted in *equation 13*, an equation for useful energy of the collector is given by.

$$Q_{coll} = A_c [G_T F_R K \tau \alpha - F_R U_L (T_c - T_a)] \quad (13)$$

Where

A_c = collector area

G_T =solar radiation

$\tau\alpha$ = Transmittance-absorption product

U_L =heat loss coefficient

T_c =collector temperature

T_a =ambient temperature

F_R =heat removal factor

The problem with *equation 13* is that it is difficult to calculate mean absorber plate temperature since it is a function of collector design. Incident solar radiation and fluid entering the collector. Therefore it is essential to formulate *equation 13* in terms of fluid inlet temperature and collector heat removal factor F_R . The equation representing the thermal performance of solar collector performance at steady conditions is given by *equation 14*.

$$Q_{coll} = A_c [G_T F_R K \tau \alpha - F_R U_L (T_s - T_a)] \quad (14)$$

This equation is known as the Hottel-Whillier-Bliss equation. As outlined by the author in reference[10], an equation for a solar thermal system with solar collector, solar pump, controller, and storage tank is given by *equation 15*.

$$(MC_p)_x = dT_{\text{---}}/dt_s = Q_u - L_s - U_s A_s [T_s - T_a] \quad (15)$$

Where

Q_u =solar-collector-generated heat input

L_s = the rate of heat removal factor

U_s =Storage tank heat loss coefficient

A_s =storage surface area

T_s =storage temperature

T_a =ambient temperature

M =storage mass

C_p =specific heat capacity of water

dT_s =change in storage temperature

dt =hourly time step

The heat from the collector depends on the collector parameters. The heat can be lost from the storage tank and be removed from the storage tank as L_s . In the first time step, the storage tank temperature (T_s) is equal to the mains temperature (T_{mains}), which is the temperature of the incoming cold water. This is because there is no heating taking place. However, after some time there will be heating. Storage temperature (T_s) which circulates heat to the collector affects how much energy flows to the system[10]. Assuming that the fluid storage tank is well mixed, T_s is the variable which depends on time.

Now T_s increases depending on how much heat is coming to the collector. As T_s increases efficiency of the collector is reduced, although total heat may increase.

This is because the amount of heat depends not only on efficiency but also on radiation which varies over a day, month and a year.

In the next time step, there is temperature storage tank temperature (T_{s+}) contents at the end finite-time –step period over which the solar thermal process is simulated (Δt) [10]. Illustrated in *equation 16*, is an equation for the temperature of storage tank contents.

$$T_{s+} = T_s + \Delta T_s \quad (16)$$

Substituting *equation 15* in *equation 16* yields

$$T_{s+} = T_s + \left(\frac{Q_{coll}}{MC\Delta t} - L\dot{s} - U_s A_s [T_s - T_a] \right) \Delta t \quad (17)$$

Which is a function of three parameters Q_{coll} , $L\dot{s}$ and $U_s A_s [T_s - T_a]$ [10]. All parameters in *equation 17* retain their meaning as in *equation 15*. Heat removal from the solar water tank to the storage tank is given by *equation 18*.

$$L\dot{s} = \dot{m}_s c_p (T_s - T_{mains}) \quad (18)$$

Where

$L\dot{s}$ = rate of heat removal from a solar storage tank

\dot{m}_s = mass flow rate

c_p = specific heat capacity of water

T_s = storage temperature

T_a = digester temperature

Maximum temperature of the load (T_{load}) to be achieved should not be more than 40°C, otherwise, this would kill microorganisms since most biodigesters work best at mesophilic temperatures [9]. If the storage temperature is greater than the

T_{mains} , heat flows from the solar storage tank into the digester. However, storage temperature should not be less than the mains temperature, if this happens the digester will lose energy since the energy will flow from the digester tank to the solar storage tank.

2.7 Factors affecting the performance of the solar thermal collector

2.7.1 Collector efficiency

Several factors affect the efficiency of the collector, they include but are not limited to, absorber coatings, reflectors, and fluids [20]. The efficiency of the collector is a variable that depends on temperature. As outlined by the author in reference [35] the efficiency of the flat plate collector is given by *equation 19*.

$$\eta_{coll} = F_R K_{\tau} \alpha - F_R U_L (T_s - G T_a) \quad (19)$$

Where

F_R =heat removal factor

$K_{\tau} \alpha$ =incident angle modifier

U_L =heat loss coefficient

T_s =storage temperature

T_a =ambient temperature

G = solar irradiance

Another equation for the efficiency of the collector is illustrated in *equation 20*.

$$\eta_{coll} = F_R \tau \alpha - F_R U_L (T_s - G T_a) \quad (20)$$

The parameters are still the same as in *equation 19*, only the incidence angle modifier has been omitted. If F_R, τ, α are assumed to be constant. The efficiency is

a linear function described by three parameters G , T_s and T_a . The slope $-F_{RUL}$ represents the rate of heat loss from the collector. Figure 7, shows the graph of collector efficiency against $\frac{T_s - T_a}{G}$ for two different collectors.

The plot of collector efficiency against $\frac{T_s - T_a}{G}$ is a straight line with a negative slope F_{RUL} representing heat loss parameter and y-intercept $F_{RT\alpha}$ is the optical efficiency of a collector. The efficiency of the collector is a variable that depends on storage temperature (T_s). As storage temperature increases, the efficiency of the collector decreases. It changes over a day.

The parameters $F_{RT\alpha}$ and F_{RUL} are found from SRCC certificate provided by the manufacture's design. As outlined in reference [10], the collector parameters $F_{RT\alpha}$ and F_{RUL} are important for predicting solar thermal performance under specific temperatures.

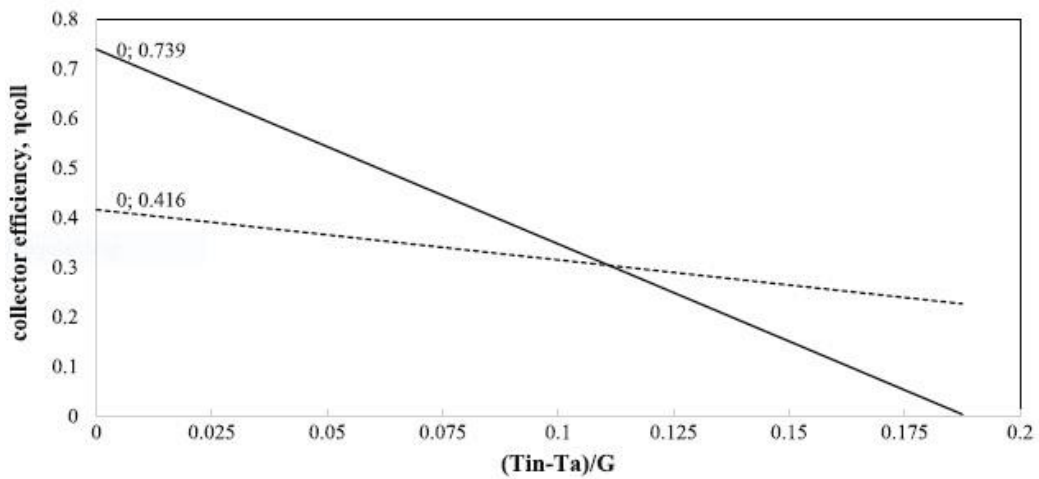


Figure 7: Collector efficiency against $(T_{in} - T_a)/G$ [10]

The solar thermal collector is chosen based on its solar performance and its costs. The more solar collectors one puts, the more the cost on each collector. The more the temperature of each collector becomes, the less efficient a collector

becomes. As outlined in reference [32], collector efficiency is higher when storage temperatures are low. On the other hand, if there is an increase in the collector area, there is less increase in the collector heat output and less increase in the production of biogas. The problem leads to optimization. There should be an optimum area for the collector area [10].

2.7.2 Incident angle modifier

Solar rating collector certificates have important parameters such as, gross area, incident angle modifier $K_{\tau\alpha}$ (IAM). Incident angle modifier is given by *equation 21*

$$IAM = \frac{1}{\cos \theta} - 1 \quad (21)$$

Illustrated in *equation 22* is an expression for $K_{\tau\alpha}$ incident angle modifier in terms of coefficients K_0 , K_1 and K_2

$$K_{\tau\alpha} = K_0 + K_1 (\cos \theta - 1) + K_2 (\cos \theta - 1)^2 \quad (22)$$

Where K_0 , K_1 and K_2 are the coefficients from SRCC data used to derive incident angle modifier function. Transmittance-absorption product ($\tau\alpha$) depends entirely on the angle of incidence of radiation. It varies from one collector to another.

Figure 8 shows the variation of $K_{\tau\alpha}$ with $\cos \theta - 1$. For a flat plane collector it can be seen that as the angle of incidence modifier $K_{\tau\alpha}$ increases the quantity $\cos \theta - 1$ decreases, while on the other hand for evacuated tube collector $K_{\tau\alpha}$ increases and

$\cos \theta - 1$ decreases. The incident angle modifier is a function of five parameters, declination angle, hour angle, latitude, longitude, and solar azimuth angle since it depends on the angle of beam radiation.

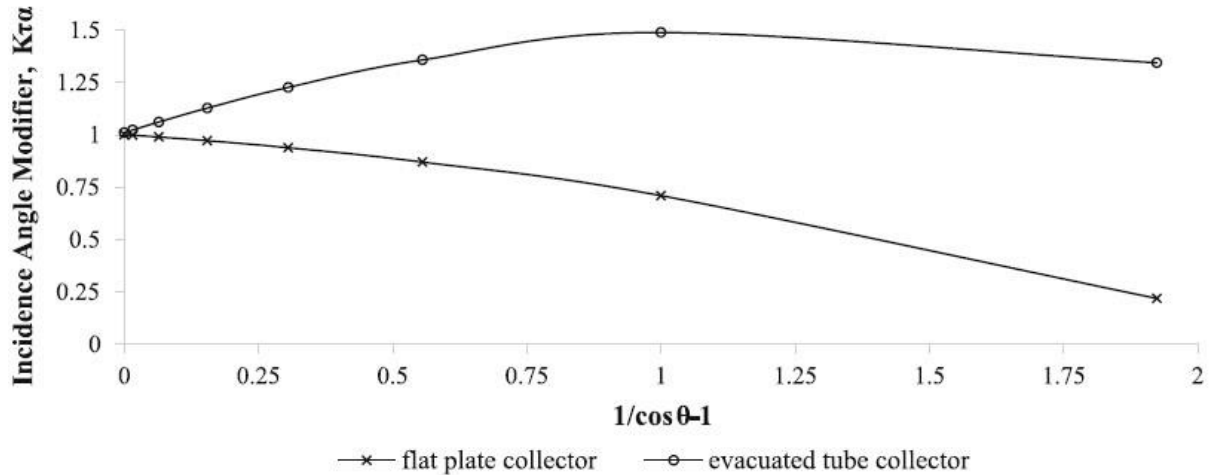


Figure 8: Variation of $K_{\tau\alpha}$ with $1/\cos\theta - 1$ for flat plate and evacuated tube collector [10]

2.8 Heat exchanger theory and capacity factor

A heat exchanger is a device that allows the efficient transfer of heat from one medium to another. Heat exchangers allow heat transfer without physical contact with the medium. There are several applications of heat exchangers in thermal industrial processes such as cooling, heating, refrigeration, air conditioning, sewage treatment, and petroleum refineries. In this research, a heat exchanger is used mainly to transfer heat between the solar thermal collector and the digester tank so that the glycol or any other liquid to be used does not mix with biodigester contents.

All heat exchangers experience capacity loss when the fluid has higher specific gravity than water. Glycol is heavy, it has to be mixed with water. However, the solution of water-glycol will be thicker than water alone. The problem is solved by introducing more surface area or a large heat exchanger. According to the author in reference [36], heat exchanger size generally affects the performance of the thermal systems. This means proper sizing of the heat exchangers has to be taken into consideration.

According to the author in reference [31], solar thermal collectors are used in combination with heat exchangers to transfer heat. The combination of solar

thermal collectors and heat exchanger works the same way as the performance of the solar thermal collectors when the heat exchanger is not be connected to the system. If the collector area is reduced the system becomes less cost-effective hence the project becomes economically viable. However the heat removal factor F_R is reduced.

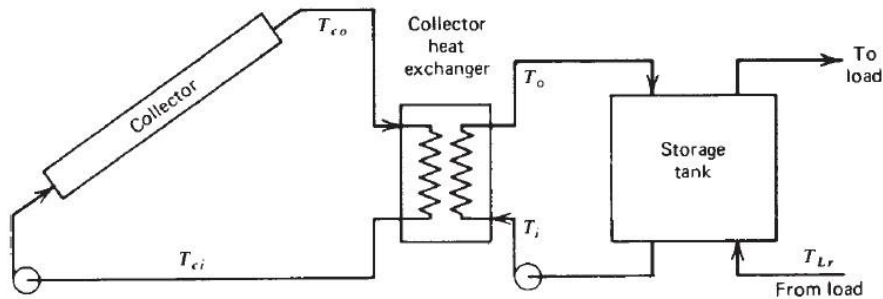


Figure 9: Schematic of a liquid system with a collector heat exchanger between collector and storage tank[28]

As outlined by the author in reference to [28], heat transfer mechanism from the solar thermal collector to the solar tank occurs by the help of the heat exchanger.

The heat exchanger correction factor F_{R1} is given by an equation 23.

$$F_{R1} = \left[1 + \frac{(A(m\dot{C}_p)_{min})}{(m\dot{C}_p)_c} (\epsilon - 1) \right]^{-1} \quad (23)$$

The heat exchanger correction factor can also be empirically determined using collector heat correction factor as a function of $(m\dot{C}_p)_{min} / (m\dot{C}_p)_c$ and

$$(m\dot{C}_p) / ACF_R U_L.$$

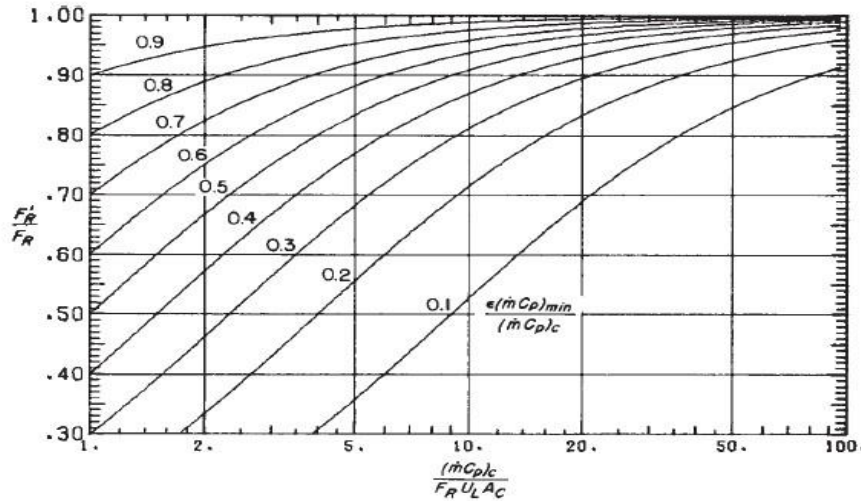


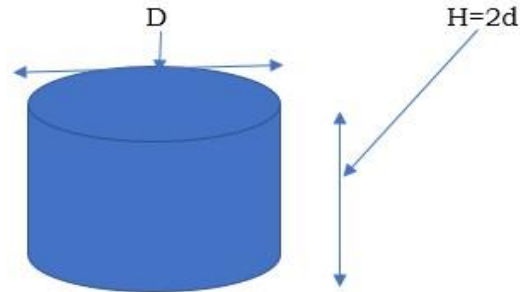
Figure 10: Heat exchanger correction factor function of $(\dot{m} C_p)_{\min} / (\dot{m} C_p)_c$ and $(\dot{m} C_p) / A_c F_R U_L [30]$

2.9.1 Temperature in a storage tank

One of the major problems with solar thermal technology is intermittence at night. The problem could be solved by introducing solar thermal storage. Solar thermal storage losses occur over the storage tank surface area. Solar thermal storage losses are proportional to the surface area of storage. Illustrated in *equation 24* is an equation for the storage tank losses.

$$S_l = U_s A_s [T_s - T_a] \quad (24)$$

Where T_s storage temperature, T_a is ambient temperature, U_s is the storage tank heat loss coefficient and A_s is the storage surface area. The storage surface area can be derived based on the underlying assumption that storage length is twice the diameter length.



The volume of a cylinder is given by $V = \pi r^2 h$ and the total surface area of the cylindrical storage tank $A = 2\pi r^2 + 2\pi r h$. But $r = \frac{d}{2}$. Expressing the surface area in terms of d , yields *equation 25*.

$$A = 2\pi \left(\frac{d}{2}\right)^2 + 2\pi \left(\frac{d}{2}\right) h \quad (25)$$

Using an assumption is that the height $h = 2d$, *equation 25* reduces to *equation 26*

$$A_s = \pi (d^2) + 2\pi(d^2) = 5\pi d^2 \quad (26)$$

Illustrated in *equation 27* is an expression for the volume of the cylinder in terms of diameter.

$$V = \pi \frac{d^3}{4} \quad (27)$$

Expressing d in terms of v and π from *equation 27* yields.

$$d = \left(\frac{4v}{\pi}\right)^{\frac{1}{3}} \quad (28)$$

Substituting *equation 28* in *equation 26* yields

$$A_s = 5.812 V_s^{\frac{2}{3}} \quad (29)$$

Where

V_s = storage volume

A_s = the storage area.

The surface area and volume of the digester are also related. It is assumed that a digester is spherical. The surface area of the digester is illustrated in *equation 30*.

$$A_s = 4\pi r^2 \quad (30)$$

Where

A_s = surface area of the sphere

r = radius of the sphere.

The volume (V_s) of the sphere is illustrated by *equation 31*.

$$V_s = \frac{4}{3}\pi r^3 \quad (31)$$

Equation 30 can be written in terms of V_s by making r the subject of the formula.

$$A_s = 4\pi \sqrt[3]{\frac{3V_s^2}{4\pi}} \quad (32)$$

A simplified form of *equation 31*

$$(33) \quad A_s = 4.835(V_s)^{\frac{2}{3}}$$

2.9.3 Economic and thermal analysis

Although solar energy resource is perpetual, the initial cost of solar thermal collector required to harness solar energy to convert it into a useful form and the storage are high [32]. On the other hand, solar thermal costs, storage tank costs and other auxiliary equipment must be known. It is very important to analyze and assess the economic viability of solar thermal technology to convince investors.

In this section, the economic and thermal analysis of the system is discussed. Several economic indicators are used to measure the economic performances of energy projects such as the payback period, LCOE, IRR, and NPV. Based on the available literature, solar thermal projects are known to have high capital costs but are cheaper in the long run [37]. It is always important to have an economic appraisal. The economic analysis compares the costs, both initial and future costs with economic benefits. In the case of the solar thermal assisted biodigester, it compares the costs of produces extra biogas as a result of increasing temperature.

2.9.4 Collector selection criteria

In this section, methods for selecting the solar collector are discussed. There are several methods used for collector selection criteria, such as energy per dollar criteria and efficient and most cost-effective collector. A study conducted by the author in reference [35] for a thermo-economic model for solar collector choice and optimal size of a solar water heater was based on energy per dollar criteria for selecting solar thermal collectors. The collector with the highest energy per dollar is chosen over a range of collectors.

On the contrary, a collector can be chosen based on the efficiency and the cost on the market. The most efficient solar collector and the one with highest energy per dollar is chosen over other solar thermal collectors.

2.9.4.1 Net Present Value calculation

The Net Present Value (NPV) is the sum of discounted cash flows subtracted from an initial investment. According to an author in reference [38], an advantage of net present value calculation is that it compares projects having different life services and different Life span. Net present value method is used to measure project cash outflows and inflows[39]. After calculating the cash flows and discounting the initial investment, revenues can be calculated.

NPV can either be negative, positive, or zero. It helps the investor in the decisionmaking process. A negative NPV shows that the project is not viable and cannot be implemented. A positive NPV shows that the project is viable, therefore it can be taken for implementation. If NPV is zero, investors cannot decide whether to go for the project or to leave project . Illustrated *Equation 34* is the formula used to calculate NPV.

$$NPV = \sum_{n=1}^i \frac{CF_n}{(1+r)^n} - I_0 \quad (34)$$

Where

CF_n = net cash flow in year n I_0 =

initial investment r = discount

rate i = economic lifetime of

investment n = year number

The discount factor is illustrated by

$$\frac{1}{(1+r)^n} \quad (35)$$

The parameter r has the same meaning as used in *equation 34*

As described by the author in reference [35], the discount rate (r) is given by *equation 36*.

$$r = \frac{(1+i)}{(1+j)} - 1 \quad (36)$$

Where

i =interest rate j =inflation

When the value of inflation is equal to the interest rate the internal rate of return is equal to zero. However, increasing the interest rate increases the discount rate, and decreasing the inflation decreases the discount rate.

2.9.4.3 Internal Rate of Return

According to the author in reference [40], the Internal Rate of Return represents the highest interest rate that an investor is willing to pay at minimum risk. An Internal Rate of Return (IRR) helps investors to know the rate of return which an investor can earn by investing in a project. It is the interest rate when the Net Present Value is equal to zero.

The general decision rule is that if the Internal Rate of Return is equal to or greater than the required rate of return the project is acceptable. If the Internal Rate of Return is less than the minimum rate of return, the project is rejected. When using the Internal Rate of Return method, the cost of capital acts as a hurdle rate that a project must be, for acceptance.

2.9.4.4 Payback Period

As outlined in reference [41], the payback period is the time required by a project to recover its initial investment. A shorter payback period (PBP) is often preferred. Since an investment project recovers its capital investment over a short period. On the other hand, payback method has a disadvantage as it pays no attention

to cash flow distribution and ignores cash flow beyond the payback period. The payback period is found by dividing the investment cost by the cash flow[42]. Illustrated in *equation 37* is an equation for the payback period.

$$PBP = \frac{Inv}{CF} \quad (37)$$

Where

Inv= Investment cost of generation

CF= cash flow achieved by annual revenues

2.9.4.5 Levelized Cost of Energy

Levelized cost of energy is the minimum price at which energy must be sold. LCOE is the cost assigned to the production of every unit of electricity. LCOE is used to compare the production of energy using other alternatives so a decision can be reached as to which method of production is the most cost-effective one. For example ,the production of electricity using fossil fuels and renewable energy technologies (RETs). Production of electricity using fossil fuel is expensive and also has negative impacts on the environment.

An easier way to determine LCOE is to do divide total life cycle cost by total Life energy production[43]. Depicted in *equation 38* is an expression for the Levelized cost of energy.

$$LCOE = \frac{\text{Total Life Cycle cost}}{\text{Total Life Energy Production}} \quad (38)$$

In addition, renewable energy technologies do not have negative environmental effects and are easy to harness. Small LCOE favors the decision-making as

opposed to large LCOE which prohibits the project from undertaken. However, the main interest is on the NPV since it measures the project life circle cost.

2.9.4.6 Benefit-Cost Ratio

Benefit-Cost Ratio is one of the key economic indicators for evaluating the viability of project investment. It takes into account capital cost, annual cost, annual income, and net annual income[44]. Net annual income is the difference between annual income and annual cost. As outlined by the author in reference [45], [46], the Benefit-Cost Ratio (BCR) is the ratio of benefits to the cost of the project investment. Illustrated in *equation 39*

$$BCRatio = \frac{\sum_{t=0}^n B_t}{\sum_{t=0}^n C_t (1+i)^{-t}} \quad (39)$$

Where

B_t =Benefit in time C_t =cost

in time

If the benefit-cost ratio is greater than 1. Then the project is economically viable.

2.9.5 Literature synthesis

In Lesotho, no study has been conducted on integrating the viability of solar thermal energy for optimizing the biogas yields for biogas plants. However, the study conducted by Gopinathan K.K on solar thermal utilization in Lesotho indicated that solar thermal devices have a potential market [1]. Another similar study was conducted by the author in reference [5]. They concluded that Lesotho has potential solar energy resources and biomass resources. However, there were no solar-assisted biodigesters in the country. Solar thermal technology and biogas technology work as isolated systems hence there is a need to study the economic viability of integrating solar thermal energy into biogas plants in Lesotho.

The production of biogas has been done by NGOs such UN, TED, and individual partners. TED has revealed that over three hundred biogases have been installed in Lesotho. However, amongst the biogas installed by the individuals, records are not available due to a lack of biomass data in Lesotho. Authors in reference [11](Italy),[6](China)February2020,[17](USA),[18](China)May2019,[14](Australia) ,[19] (Morocco), and [47] (China) 2011 have investigated the performance of solar-assisted biogas digester. They found that temperature can greatly affect the performance of solar-assisted biodigesters.

However, the authors in reference [48] were specific in their findings. They highlighted that for two digesters one fitted with solar thermal energy and the other without solar thermal energy at an average temperatures of 9.5 °C and 4.9 °C respectively. The corresponding volumes of biogas produced were 357 L/m³day 300 L/m³day [48]. However, the volume of the digester was not specified.

There is a similarity between the study conducted by authors in reference [6] and [17], however, the two studies did not cover the aspect of the economic viability of integrated solar-assisted solar thermal technology. Authors in references [17] and [19] had similar findings different from authors in reference [49]. Their results revealed that the solar-assisted biogas produced more biogas than non-solar biogas digester. On the other hand author [50], had investigated the feasibility of integrating solar thermal into biodigester through the use of electricity and heat pumps. The results indicated that the system does not work well with the mesophilic condition. Secondly, removal of the heat pump does not cause the required temperature to drop out of the mesophilic conditions.

Similar studies were performed by authors in reference [51],[52],[53],[19],[54], and [14] on investigating the viability of using solar thermal technology for optimizing the biogas yield. In Italy, the author in reference [51] used an organic fraction of municipal wastes (OFMSW) integrated with using solar thermal collectors to produce biogas to analyze a community generation system. Results revealed that a system is sustainable when renewable sources of energy are used.

The author in reference [53], investigated on conditions and performance of lowcost tubular digesters for biogas production using passive heating. The results showed that passive solar heating increases the slurry temperature above the ambient temperature. It was concluded that biogas production of $0.2m^3/m^3d$ was produced.

In Morocco, the authors in reference [19] develop a solar-assisted biodigester to make the country's energy sufficient. The system was modeled using an up-flow anaerobic sludge blanket (UASB) coupled with the TRNSYS platform. It was discovered that, the developed model could predict an optimal size of solar water heating systems and digester. Their conclusion highlighted that solar thermal energy improves the performance of biodigester by increasing digester temperatures. However, they recommended that future research should focus on the economic viability of the production of biogas as most of the researches done focused mainly on experimental investigation.

The author in reference [18], investigated biogas production to promote multiframe technology and biogas production. It was concluded that thermal energy is one of the factors which enhances the effectiveness of biogas production. It was also found that a $12m^3$ biodigester produces $0.63m^3/m^3 d$ at temperature of $27.2^\circ C$. In addition the optimized solar thermal system and the economic appraisal of the system were found.

Furthermore, the authors in references[55],[11],[56],[57] had assessed the economic viability of using solar thermal energy to effectively enhances the production of biogas production using the economic performance indicators such as Payback Period (BPC), Net Present Value (NPV), Internal Rate of Return and Benefit-Cost Ratio (BCR). The authors in reference [55] found out that when the solar thermal energy is installed to the $9000m^3$ biodigester, the results show that the project is economically viable with a positive NPV, payback period of 5 years, and discount rate of 23 %.

The authors in reference [11] had similar findings as authors in reference [51] that the project is economically viable, however, pointed out that the project

becomes economically viable when less expensive collectors are used. The project payback was found to be more than 10 years. Moreover, the research conducted by the authors in the reference [56] and [57] agreed with the findings. The authors in reference [56] found out the payback period of 11 years with a positive NPV and minimum profits.

The reviewed literature shows that as much as solar thermal energy greatly affects the production of biogas production. The economic viability of using solar thermal energy in biogas production has not been addressed in Lesotho. There is a need to investigate the economic viability of using solar thermal technology. Hence there is a need to effectively carry out the study in Lesotho.

This section dealt with the literature review on the work that has been done on the techno-economic viability of solar thermal energy for optimizing gas yields for biogas plant.

The next section will look into the method on the research topic and the details on how the results of the study are obtained.

3.0 Materials and Methods

The purpose of this section is to respond to the research questions which states that, is it economically viable to use solar thermal energy to enhance the effectiveness of biogas digestion? And to what extent is the solar thermal energy deployment (number of solar collectors) in a biodigester system? In response to these questions. This section focuses on the research methods that will be employed for investigating the viability of integrating solar thermal energy for optimizing the gas yields for biogas in Lesotho.

A comprehensive analysis of the model used in the study is well explained as well as reasons behind chosen a model over other models. As discussed in section two, TMY data has been used to develop the model. TMY data gives the solar radiation on an hourly basis while Collares-Pereira and Rabl model assumes the

monthly averages of each day. TMY data is used since it gives data on an hourly basis since the position of the sun on the sky varies hourly over the day.

3.1 Microsoft excel model

Microsoft excel model was developed to carry out system analysis and performances. The model requires geometrical data such as latitude and longitude, tilt angle, and surface azimuth. Location for a selected place of study was taken at latitude -29.2° and longitude 27.7° . Solar surface azimuth angle was taken as 180° . The model is location-specific because of geometric coordinates and is able to predict solar thermal performance and economic analysis at any location at different times of the day and the year in Lesotho.

The model uses TMY data and collector parameters as the inputs. Both collector area and collector parameters $F_{RT\alpha}$ and F_{RU} were placed in the model. The solar storage surface area and the digester surface area are calculated using *equation 29 and equation 33*. System temperatures and thermal energy outputs are observed each time the solar collector area is varied to decide which collector area will give maximum NPV. A collector was chosen based on the energy per dollar criteria. NPV will be calculated using *equation 39 section two*. Each time the collector area is varied, collector area, NPV, and volume of biogas produced are observed. The collector which gives the highest NPV is considered as the best collector which will then be used to optimize the system.

Using the prevailing interest rate and prevailing inflation rate, the economic viability of the integrated solar thermal assisted biogas is assessed. The discount rate is calculated using *equation 36 in section two*. The model further looks at comparing the benefits of producing biogas with other sources of energy. Environmental benefits such as greenhouse gases averted are calculated from the excel based program.

3.2 Solar radiation inputs and assumptions

Based on the available literature, TMY data is essential for conducting solar thermal analysis systems [58]. TMY data provides hourly solar irradiance, temperature, wind speed, and humidity [19]. Solar radiation data is available on a horizontal surface which can be modeled to produce radiation on a tilted surface. The solar thermal collectors do not see the radiation on a horizontal surface. It is therefore important to model radiation on a horizontal surface to a tilted surface using tilted plane models. Global radiation (I_h) and the diffuse radiation (I_d) will be obtained from the TMY data. Beam radiation will be found by inference using the *equation 1*. TMY data is used since it is already giving solar radiation on an hourly basis. The tilt angle β is obtained by taking the absolute value of latitude angle φ , plus 5° [10]. The corrected latitude angle is given by *equation 40*.

$$|\varphi| + 5^\circ \quad (40)$$

3.3 Determination of solar radiation on a tilted surface

Determining radiation on a tilted surface I_t , the following solar geometrical inputs; day number (N), declination angle (δ), $\cos\theta_z$, $\sin\theta_z$ solar azimuth (γ_s), $\cos\theta$ and beam radiation (R_b) were calculated. Declination angle (δ) was calculated using *equation 8*, $\cos\theta_z$ was obtained using *equation 6*, and $\sin\theta_z$ was obtained *equation 7*. Other geometrical inputs such as solar azimuth (γ_s), hour angle (ω), $\cos\theta$ and beam radiation (R_b) were obtained using *equation 9*, *equation 5*, and *equation 3* respectively.

The assumption is that the collector is in the southern hemisphere and is facing to the north with the surface azimuth, $\square = 180^\circ$, *equation 4* in *section 2* becomes an equation for $\cos\theta_{equator}$. Illustrated in *equation 41*, is an equation for $\cos\theta_{equator}$ used to calculate the angle of incidence of beam radiation.

$$\cos\theta_{eq} = \sin\delta\sin(\varphi + \beta) + \cos\delta\cos(\varphi + \beta)\cos\omega \quad (41)$$

Parameters retain their usual meaning as in *equation 4 section 2*. The solar radiation inputs are placed in *equation 2 section two* to determine the radiation on the tilted surface.

3.4 Other system inputs

Additional system inputs such as the value of biogas, the density of biogas, and greenhouse gases averted were also obtained from the literature. The calorific value of biogas is around 38.8 MJ/ m³[59],[17].Density of biogas is 1.15kg/m³ at standard temperature and pressure [60].It has been said from the literature that the use of biogas replaces 1.7 CO₂/ kg for wood, 3.45 kg CO₂/ kg for coal, 2.5 kg CO₂kg /L for kerosene, and 1.9 kg CO₂/L of LPG

<https://irena.org/newsroom/articles/2017/Mar/Biogas-Cost-Reductions-toBoost-Sustainable-Transport>.Using the value of one cubic meter biogas, energy produced from the biogas can be calculated for any volume produced by the biogas since the volume of the digester is known to be 5m³.

Economic inputs such as collector costs and collector warranty are obtained from the market. Interest rate and inflation rate are taken as prevailing interest and the prevailing inflation. The prevailing interest rate and the prevailing inflation rate are taken as 8.56% and 4.9% respectively <http://www.centralbank.org.ls/index.pnp/statistics>.

The discount rate is calculated as a function of inflation and interest rate using *equation 36*. The inflation rate and interest rate are taken as the average of the past months.The discount factor is calculated using *equation 35* using the prevailing interest and prevailing inflation.The Net Present Value is then calculated using *equation 34*, since it depends on the discount factor given by an *equation 35*.

Collector costs and storage costs are found at <http://www.alibaba.com>. The price of the collector and the storage tank are found in the market and placed in the excel program. This is done for ten collectors which are chosen. A collector with the maximum NPV is taken as the best collector. Other system inputs such as greenhouse emission factors are placed in the excel model. The calculations are performed in an hourly time step since the solar radiation is available on an hourly basis.

The Benefit Cost Ratio (BCR) is calculated by dividing the Present Value of the benefits and Present Value of the costs, using the discount factor for every year for the period of twenty years as illustrated in *equation 39 section two*.

3.5 Description of the model used for integration of solar thermal into biogas

Equations of solar thermal integrated biogas model were developed based on the proposed model using energy balance of the system. Figure 11 shows the schematic diagram for the designed system. The system is a closed circulation system with a solar thermal collector for converting solar radiation into thermal energy. Solar storage tank for storing heat that goes to the digester and digester tank to store the liquid waste.

Two heat exchangers one for transferring heat down the storage tank and the other to transfer heat between the storage tank and digester tank. Lastly, the circulation pump, to pump the liquid from the storage tank to the collectors. The thermal energy input energy of the collector will be calculated using *equation 14 section two*.

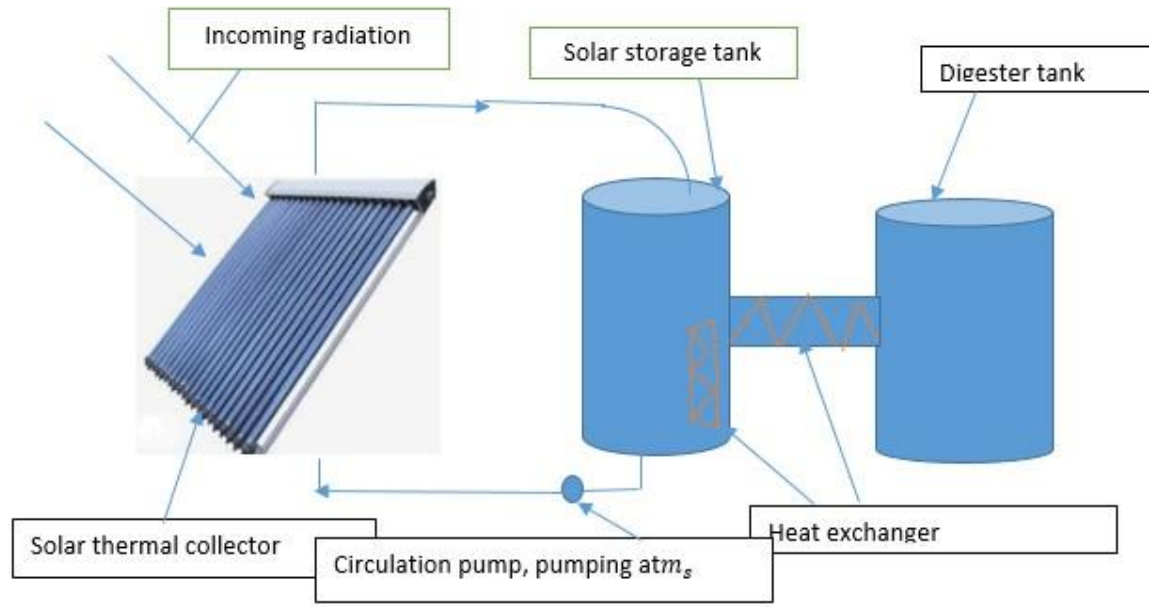


Figure 11: Proposed schematic for solar integrated bio digester system

3.6 Energy balance of solar water storage

The initial storage temperature (T_s) for the model, was assumed to be equal to the mains temperature (T_{mains}) since there is no heating taking place.

$$T_{mains} = 0.57T_a + 6.8 \quad (42)$$

Parameter T_a has the same meaning as in *equation 19*. The assumption is that the temperature of the cold water entering the solar water heating system is equal to the temperatures of the mains since the pipe is buried in the soil [18].

There is a correlation between ambient temperature and temperature of the soil [61].

However, after some time there will be heating, as T_s increases depending on how much heat is coming to the collector. The temperature of solar storage tank contents at end of the finite time-step is given by *equation 43*

$$T_{s^+} = T_s + \Delta T_s \quad (43)$$

Where

T_{s^+} = incoming temperature

But a change in storage temperature ΔT_s is given by *equation 44*

$$\Delta T_s = \left(\frac{Q - L - U_s A_s (T_s - T_a)}{m c \Delta t_p} \right) \Delta t_p \quad (44)$$

Equation 43 can be written in terms of Q , L and $U_s A_s (T_s - T_a)$ as

$$T_{s^+} = T_s + \left(\frac{Q - L - U_s A_s (T_s - T_a)}{m c \Delta t_p} \right) \Delta t_p \quad (45)$$

Parameters still retain their usual meaning as used in the previous equations.

In order to calculate Q , the collector parameters $F_{RT\alpha}$, F_{RU_L} , $K_{\tau\alpha}$, net area, and cross-area were obtained from solar rating and certificate of corporation.

The first equation of energy balance is the equation that shows heat gained by the solar tank. The rate of change of temperature is expressed in terms of the energy balance of the tank. The rate of change of internal energy of a system is given by *Equation 46*

$$M_s \times C_p \times \frac{dT}{dt} = Q_{coll} - L_s - U_s A_s (T_s - T_a) \quad (46)$$

Equation 45 can be written using Euler integration by replacing dT_s by ΔT_s and dt by Δt . Making ΔT_s in Equation 45 subject of the formula the new equation for ΔT_s is given by Equation 47.

$$\Delta T_s = \frac{Q_{coll} - L_s - U_s A_s (T_s - T_a)}{M_s \times C_p} \quad (47)$$

Where

M_s =storage mass

C_p =specific heat capacity

Q_{coll} =collector energy output

$U_s A_s$ =storage losses

T_a =ambient temperature

T_d =digester temperature

The efficiency of the collector was found using equation 17 section two. Solar thermal storage heat losses were found using equation 21 in section two.

3.7 Energy balance of the digester

The second equation of energy balance is an equation between the storage tank and the digester tank. Depicted in equation 48 is an equation for energy balance for the digester tank and storage tank.

$$M \times C_p \Delta T_d = (L_s - U_d A_d (T_d - T_{mains})) \quad (48)$$

Equation 47 can also be written using the Euler integration form.

$$\Delta T_d = M \frac{\Delta t c_p}{\Delta t} ((L_s - U_d A_d (T_d - T_{mains}))) \quad (49)$$

Where

L_s = heat extraction from the solar storage tank

T_{mains} = storage temperature

T_d = digester temperature

U_d = digester heat losses

A_d = the surface area of the brick building a digester tank.

T_a = the ambient temperature

M = storage mass

Δt = hourly time step

The equation relating the digester temperature and volume of biogas produced when the solar thermal collectors are installed, was found by taking values of temperature and volume of biogas produced in reference[18]. The points were trend fitted to give a second-order polynomial. Figure 12 is the graph that shows the relation between the digester temperature and the volume of the biogas produced. The graph shows the volume of the biogas produced at different digester temperatures. Illustrated in *equation 50* in an equation that gives the volume of the biogas production at any particular value of the digester temperature.

$$V_{biogas} = -0.001 T_d^2 + 0.0164 T_d + 0.0399 \quad (50)$$

Where

V_{biogas} = volume of biogas

T_d =digester temperature

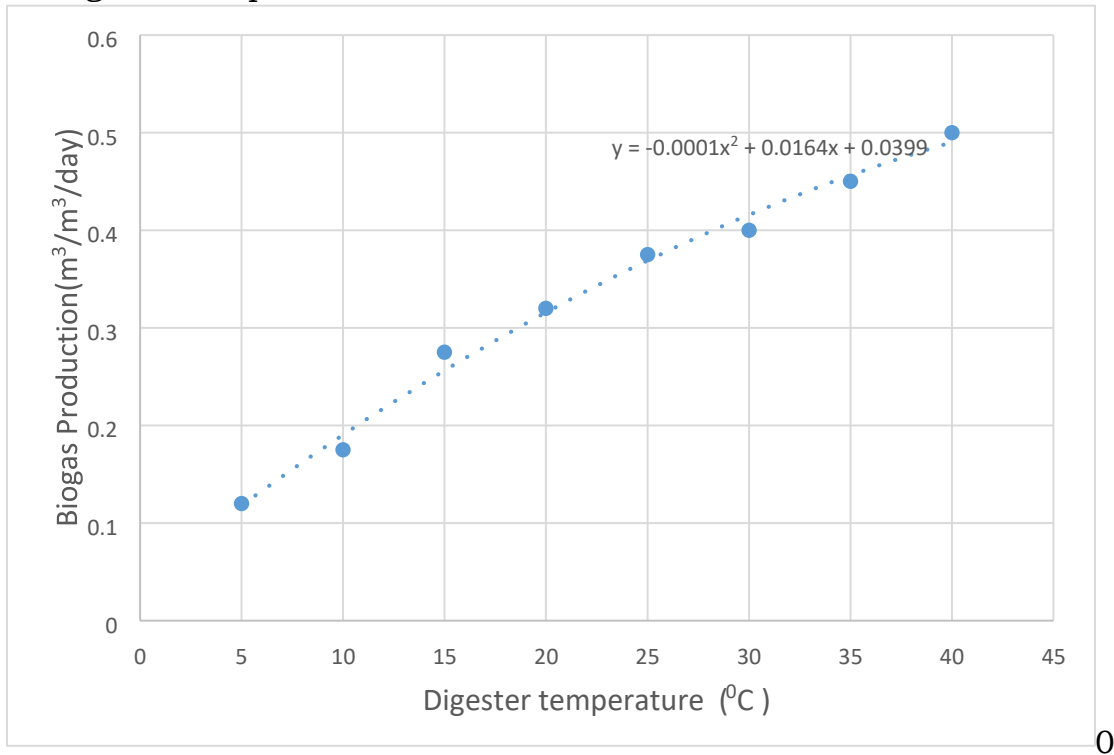


Figure 12: Digester temperature against the volume of biogas produced

As discussed in the previous section that all other parameters except temperatures are constant and optimized. The type of feedstock in used in this research is pig manure. When all the conditions are all optimized, the PH of the feedstock is 7.0, the retention time is one day and the working pressure is 760mm Hg.

3.8 Sizing the solar thermal storage

Due to the variability of solar energy resources and their intermittency, it is important to have solar thermal storage so that there is enough energy stored to operate load when there is no sun at night or on cloudy days. Nevertheless, It is not cost-effective to provide 100% of solar thermal energy all year round as it would result in an oversized system[32].

The author in reference [10] in the article entitled: a thermo economic model for aiding solar collector choice and optimal sizing for solar water heating system

developed a model in Zimbabwe. The same model can be used for sizing the solar thermal storage tank in Lesotho. The author pointed out that the solar storage tank size is equal to the collector area divided by $18m^2/m^3$ [11]. Illustrated in *equation 51*, is an equation for calculating storage size for the solar water heater in Zimbabwe which can also be applied in Lesotho.

$$\text{Storage size} = \text{Collector} \frac{\text{Area}}{18 \text{ m}^2/\text{m}^3} \text{ (m}^3\text{)} \quad (51)$$

The volume of the digester is known to be $5m^3$ which is equivalent to the mass of 5000kg. The mass flow rate to the digester can be found by dividing the mass of the digester by the number of hours in a day. Illustrated in *equation 52* is an equation for the mass flow rates.

$$m_s = 24 \frac{M}{3600} \quad (52)$$

Where

m_s =mass flow rate in kilogram per hour

M= Mass of digester in kilogram

The storage size will vary according to the collector size. The storage is determined by the size of the collector used. It is assumed that the energy demand of the digester is similar to that of the residential system as described by the author in reference[10].

As the collector area increases the storage volume and surface area increases as well. Figure 13 shows the graph of collector area, storage volume, and storage surface. In this case, the graph of the collector area against storage volume is a straight line which shows that there is a linear relation between storage volume

and the collector area. However, for storage surface area, the graph is not a linear function, as the collector area increases the surface area decreases.

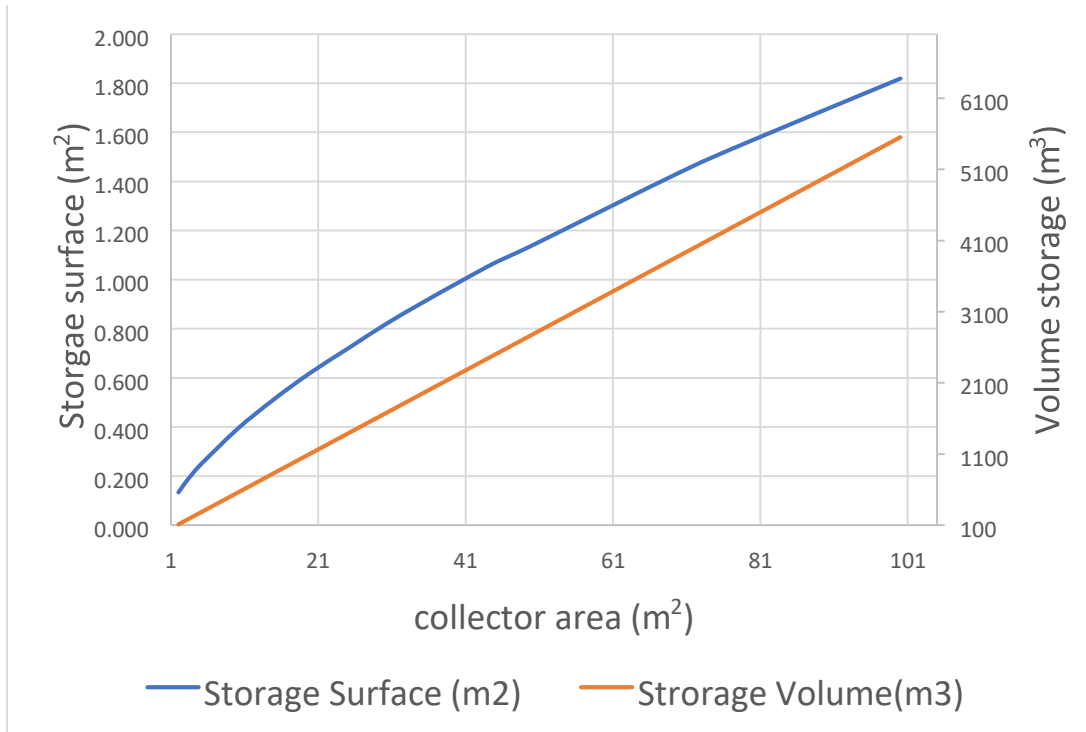


Figure 13: Collector area, storage surface, and storage volume

On the other, as the collector area increases storage surfaces increase and then decrease, which indicates that the relationship between a storage surface area and collector area is not a linear function. There is an optimum storage surface to be determined. The heat that goes to the digester is the heat extracted from the solar storage tank. Heat to the digester is calculated using equation 18 *section two* taking into account that the energy demand of the digester is the same as that of the residential system.

The digester load temperature should not be more than 40°C since the production of biogas is optimum at a mesophilic temperature. The annual average mains temperature was obtained as 16°C.

3.9 Collector selection criterion.

Solar thermal system inputs parameters were obtained using *equation 18* up to *equation 33*. Collector input parameters gross area, optical efficiency, and heat loss parameters were obtained from solar rating certificates of a corporation which was obtained at www.srcc.directory.

Five flat plate collectors and five evacuated tube collectors were obtained from solar rating certificate web site. For each collector, angle of incidence modifier

$K\tau\alpha$ and $\frac{1}{\cos(\theta)} - 1$ was determined. Graph of incidence angle modifier against $\frac{1}{\cos(\theta)} - 1$ was plotted and trend fitted to give second-order polynomial. Coefficients K_0, K_1 and K_2 were determined from the second order polynomial for every solar thermal collector. However, *equation 19* which involves the uses of the collector parameters described is not used. Instead, *equation 20* which calculates the efficiency of the collector without angle incidence modifier was used. This is because the calculation of $K\tau\alpha$ in *equation 19* is cumbersome and time-consuming. The solar thermal collectors were ranked using energy per dollar matrix as outlined by the author in reference[10].

Coefficients K_0, K_1 and K_2 were determined from the second order polynomial for every solar thermal collector. However, *equation 19* which involves the uses of the collector parameters described is not used. Instead, *equation 20* which calculates the efficiency of the collector without angle incidence modifier was used. This is because the calculation of $K\tau\alpha$ in *equation 19* is cumbersome and time-consuming. The solar thermal collectors were ranked using energy per dollar matrix as outlined by the author in reference[10].

Table 1 and figure 14 and figure 15 shows how the coefficients of the evacuated tube collector and flat plate collector were determined as an example. From table 1, the angle θ was converted into radians and then used to calculate

$\frac{1}{\cos(\theta)} - 1$ for Thermpower evacuated tube collector and Apricus flat plate

Collector using the excel model. The exercise was carried out ten times for each of the collectors which were chosen.

Table 1: Relationship between angle of incident of beam and incident angle modifier

Thermo Power (ETC)			Apricus (FPC)		
θ	$1/\cos(\theta)-1$	$K\tau\alpha$	θ	$1/\cos(\theta)-1$	$K\tau\alpha$

10	0.02	1.02	10	0.02	1.02
20	0.06	1.07	20	0.06	1.07
30	0.15	1.16	30	0.12	1.17
40	0.31	1.29	40	0.30	1.3
50	0.56	1.25	50	0.56	1.43
60	1.00	1.54	60	1.00	1.43

Figure 14 and figure 15 shows the graphs obtained from the plot $K\tau\alpha$ and $\frac{1}{\cos \text{Rad}(\theta)} - 1$ to give the second order polynomial which were used to determine

the coefficients k_0 , k_1 and k_2 . Thus for the two collectors ;thermopower (ETC) and Apricus (FPC) the coefficients k_0 , k_1 and k_2 were found to be 1.003, 1.135 and 0.5957 for thermpower and 1.0018, -0,284 and 0.053 for appricus respectively.

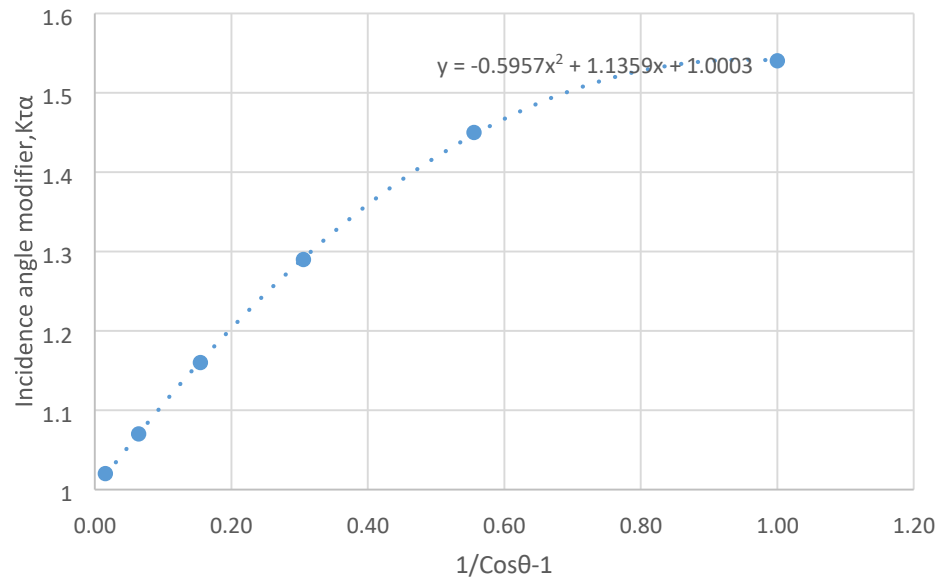


Figure 14: Coefficients for Evacuated Tube collector

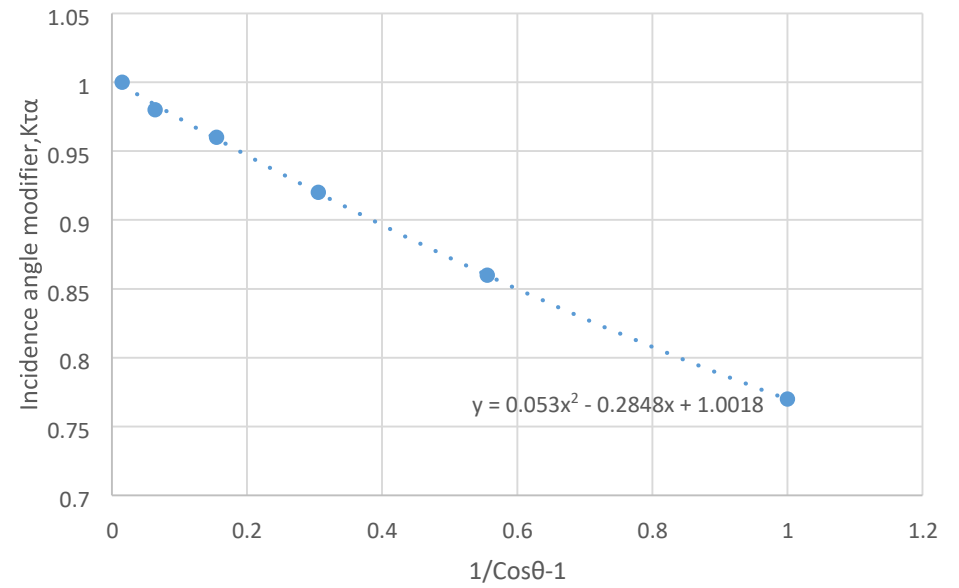


Figure 15: Coefficients for Flat Plate collector

All ten types of collectors ,five flat plate collectors and five evacuated tube collectors were ranked using an energy per dollar matrix. This is a decisionmaking matrix used to select a solar thermal collector with the highest energy per dollar. Energy per dollar is a suitable metric used to compare the level of cost-effectiveness of different collector sizes. The metric divides the collector average annual yield by the annualized life-cycle (warrant period) cost at the sweet spot collector area.

The collector area was varied and each time the collector area was varied, the Net Present Value was observed. The energy per dollar was calculated for each collector at maximum NPV. The collector with the highest energy per dollar was chosen as the best collector. The collector was placed in the model and the simulation was performed to obtain optimum collector area. The optimum collector area was the one that predicts the system design. Collectors were ranked in order of decreasing order of energy per dollar, starting with the collector that has highest energy per dollar .

Flat plate collectors (FPC) are generally good for solar water heating systems since they have high optical efficiency, but, their cost in the market is relatively higher compared to the evacuated tube collectors (ETC). The latter have low optical efficiency, low heat loss parameter, and their cost are generally low compared to the flat plate collectors.

Collectors are sold at a cost per square meter. The cost per square meter of each collector is obtained by dividing the total cost of each collector by cross area. The calculations are simulated on an hourly time step. The project profitability indices are calculated from *equation 34* to *equation 39*.

In *section three* a general overview of method used to investigate the viability of solar assisted biogas was dealt with. The next section will deal with the disussions of the findings obtained from *section three*.

4.0 Results and discussions

This chapter presents the results for modeling solar radiation on a tilted surface, selection of solar thermal collectors, system sizing, optimization of the results, and economic analysis. It will further look into the annual production of biogas when solar thermal energy is used to the enhancement biogas. It is worth noting that both solar thermal performance and economic performance indicators are key parameters in analyzing the economic viability of the project. Economic indicators which assess the viability of the project such as Net Present Value, project Payback Period, Internal Rate of Return, and Benefit-Cost Ratio will be unpacked in this section.

The selected solar thermal collectors are ranked in using energy per dollar matrix as shown in table 2. From the table 2, it can be seen that flat plate collectors (FPC) have high optical efficiency, low heat loss parameter, and high cost compared to the evacuated collectors (ETC). The latter have low optical efficiency, low heat loss parameter, and low cost.

Sun power (ETC) is found to be the best collectors amongst the ten collectors. Sun power is ranked number 1, with the energy per dollar of $25.3kWh/\$$, the area of 19 per metre cube, the solar fraction of 90 and warranty of five years. It is chosen because it has the highest energy per dollar compared to other collectors.

The sun power collector optical efficiency ($F_{RT\alpha}$) is 0.442 and heat loss parameter (F_{RUL}) is 1.501 with the cross area of $3.815m^2$ and collector warranty of 5 years, which means it can still perform well even after five years. This collector has high energy per dollar, low optical efficiency but low heat loss parameter so

it does not lose heat quickly that is why it is suitable for the design system. Moreover, it suits system optimization since it has high energy per dollar as compared to other solar thermal collectors. The Sunpower solar thermal collector outcompetes all the other chosen collectors, hence it is the one to be considered for system optimization.

Table 2: Solar thermal collector ranking using energy per dollar criterion

Ranking solar thermal collectors													
Model	Type	Cost/m ²	Intercept	Slope	Ko	K1	K2	Gross Area (m ²)	Warranty	Energy/\$	Area/m ³	Solar Fraction	Price(\$)
Sunpower	ETC	58.38	0.422	1.501	1	0	0	3.815	5	25.3	19	0.9	223
Apricus	ETC	150.30	0.441	1.506	1	1.21	0.78	2.994	15	18.2	23.7	0.89	450
Titan Power Plus	FPC	478.42	0.747	-4.38	1	-0.3	0.02	2.176	10	18	23.7	0.88	1041
Duda Solar	ETC	1216.67	0.442	0.786	2.3	4.91	1.83	4.666	10	17.2	32.9	0.946	5677
Sun bank	FPC	204.19	0.767	4.346	1	-0.2	0	3.913	10	16	20.7	0.84	799
Thermo Ray	FPC	427.21	0.74	4.115	1.1	3.09	1.15	2.31	5	15.9	22.9	0.88	987
Heliodyne Gobi	FPC	412.8	0.767	4.346	1.4	3.54	1.32	3.193	10	15.8	22.9	0.78	1318
Thermo Power	ETC	286.20	0.406	1.753	1	1.14	-0.6	5.241	10	14.8	23.9	0.89	1500
Hydrosol	ETC	320.67	0.422	0.786	2.3	4.91	1.83	2.342	10	11.5	46.5	0.89	751
SUNRAIN	FPC	399.5	0.679	4.653	2.4	5.14	1.91	2	5	8.8	27.6	0.89	799

Comparing angle of incidence of beam radiation and reflected beam radiation.

Figure 16 shows the variation of the angle of incidence of beam radiation ($\text{Cos}\theta$) and the reflected radiation (R_b). It can be seen that the angle of beam radiation is negative in the morning hours before the sunrise and negative in the afternoon hours after the sunset. It increases when the sun rises and decreases during the sunset. It is also maximum and symmetrical at noon. It is also maximum and symmetrical at noon.

The reflected radiation is zero in the morning hours before sunrise. It increases rapidly after the sunrise compared to the angle of beam radiation. Both reflected radiation and the angle of incidence of beam radiation decrease in the evening hours at the sunset.

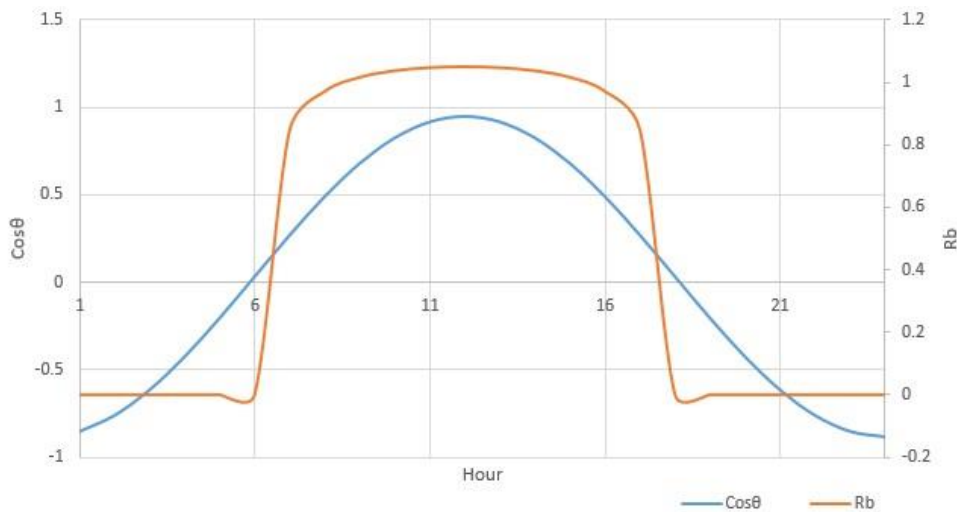


Figure 16: Variation of the angle of incidence beam radiation and reflected radiation

The angle of incidence of beam radiation influences the system performance. Figure 17 shows the graph of radiation on a tilted surface and the collector energy output. There is no radiation and collector energy output in the morning hours before sunrise as well as evening in the hours when the sunsets. However, the two graphs are skewed, one to the right side and the other to the left side since the graphs are obtained from the scientific models which are based on the assumptions. Both collector energy output and radiation on the tilted surface are symmetrical at noon. The maximum radiation received by the collector is around $1100\text{W}/\text{m}^2$ while the maximum collector energy is around 61000J .

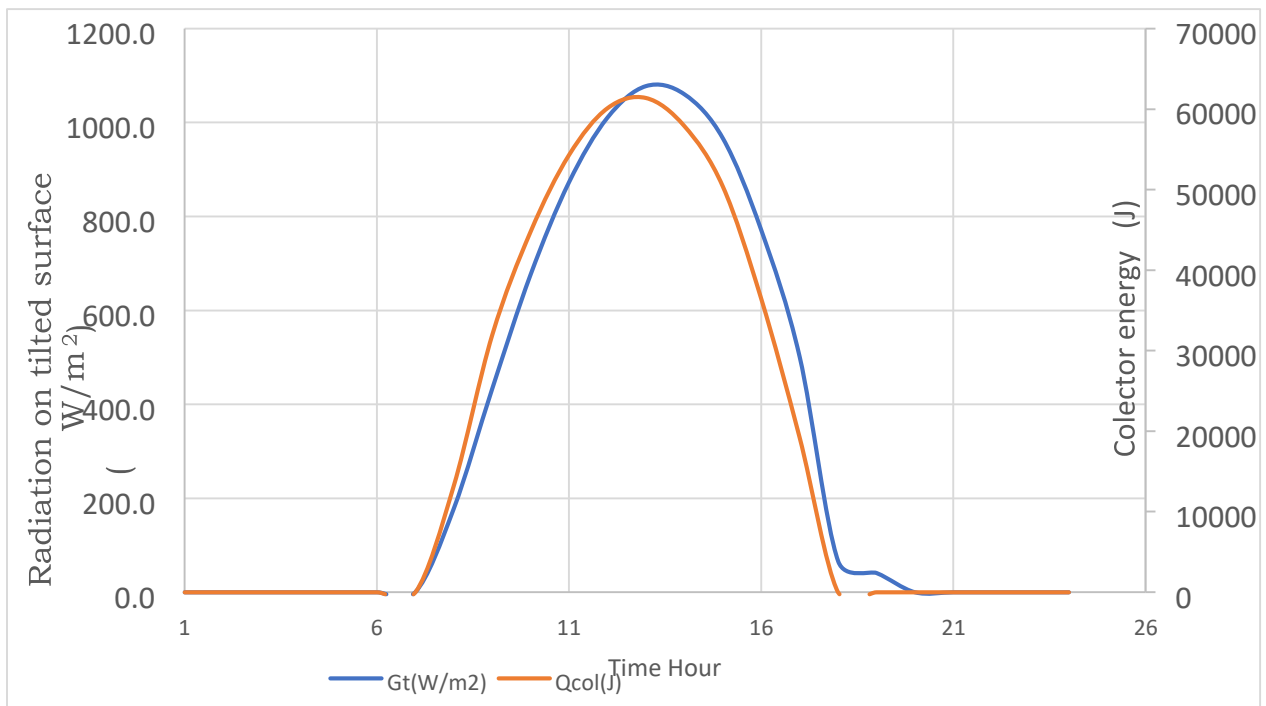


Figure 17 :Variation of radiation on a tilted surface and collector energy output
Comparing collector energy output and collector efficiency.

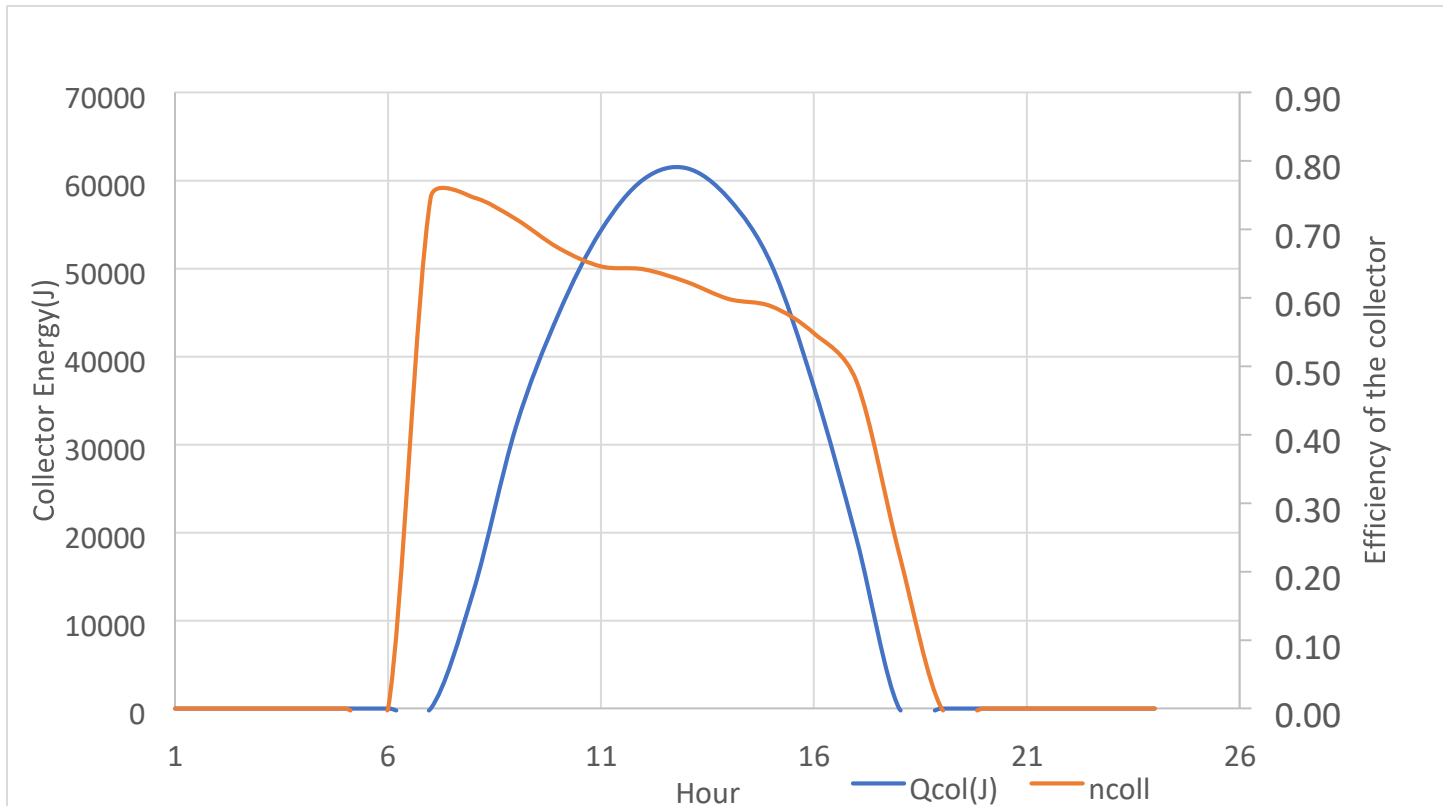
As outlined in *section two* efficiency of the collector is a function of solar irradiance (G), thermal optical efficiency ($F_{RT}\alpha$) and storage temperature (T_s). When the collector energy increases, storage temperature increases but the

efficiency of the collector decreases. The thermal collector efficiency (η_{coll}) should not be more than the solar thermal optical efficiency ($F_{RT}\alpha$).

Figure 18 shows the collector energy and the collector efficiency graph. From the graph, it can be seen that the maximum thermal collector efficiency achieved is 0.75 which starts in the morning hours around 0600hrs when the sun rises. The efficiency decreases as the collector energy increases from 0600hrs to 1900hrs where it reaches zero since there was no energy supplied by the collector.

Figure 18: Variation of collector energy and efficiency over a day
System temperatures and biogas volume

The collector energy output and efficiency of the collector affect the system



temperatures and its performance. Figure19 shows how the system

temperatures vary during the day. It can be seen that the mains temperature is 14°C in the morning hours. It increases from 14°C and reaches 28°C at 1500hrs in the evening. The mains temperature increases in the morning hours from 0600hrs when the sun rises. Its value is around 28°C at 1530hrs in the afternoon hours. It then starts to decrease from 1530hrs in the afternoon hours till at night.

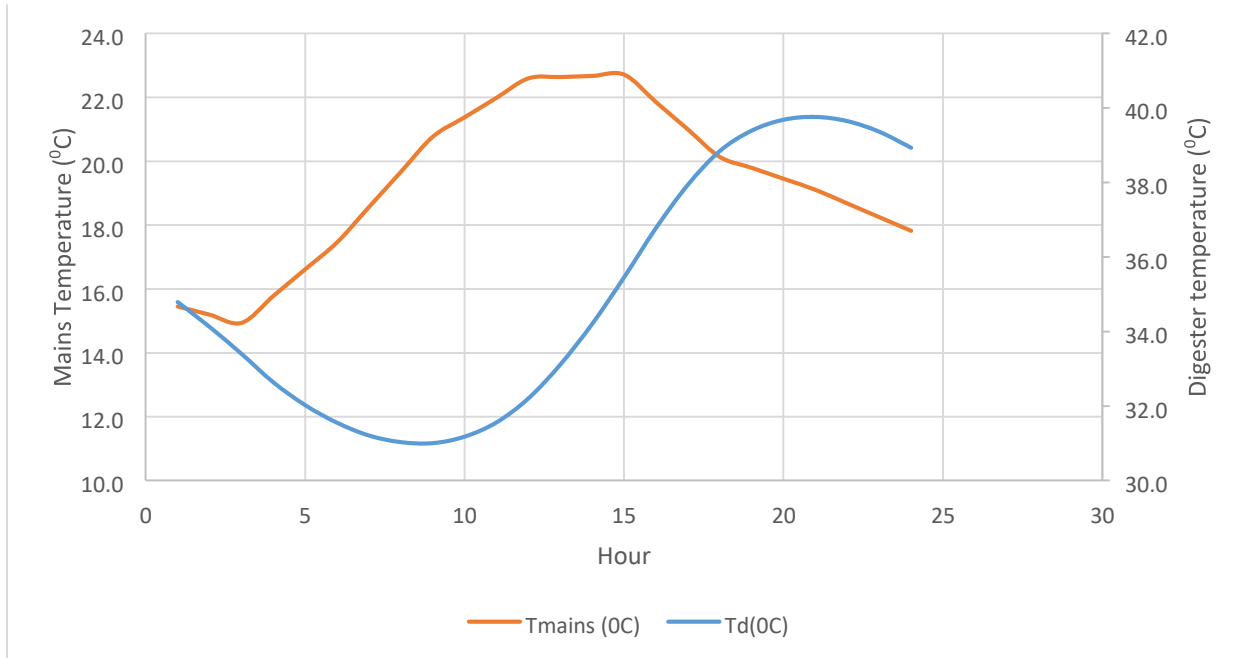


Figure 19: System temperatures

The change in storage temperatures results in a change in system temperatures and biogas production. From the figure, it can be seen that both mains temperature and digester temperature are not linear functions. The mains temperature is minimum at night when there is no radiation. It is 14.8°C at 0500hours in the morning hours. It increases from 0500hrs until it reaches a

maximum of $22.70^{\circ}C$ at 1500hrs in the afternoon hours. It then decreases from 1500hrs until at night.

On the other hand, digester temperature (T_d) starts to increase in the morning hours at 0800 hours when there is solar energy supplied by the solar thermal collectors. It increases from 0800hrs to till 1800hrs where it starts to decrease until at night since there is no solar thermal energy available. The digester temperatures decrease at night until morning hours because of heat extraction(L_s) from the solar storage tank to the digester. During heat extraction the storage temperature decreases. The heat transfer temperature is then pumped back to the solar thermal collectors at lower temperature than it had before. The lower temperatures helps to improve the efficiency of the solar thermal collectors.

From the graph, it can be depicted that the rate of heat loss by the digester is low since the digester does not lose much of the solar thermal energy it has absorbed. The digester is made up of bricks with a heat loss coefficient of $0.5 W/m^2 /C$ [62].

System temperatures and biogas volume

Figure 20 shows the volume of biogas produced when there is solar thermal energy supplied to heat the digester and the volume of the biogas when there is no solar thermal energy supplied. From the figure, the volume of biogas produced without solar thermal (bws) that is under normal operating conditions ranges from $0.062m^3/m^3/day$ to $0.072m^3/m^3/day$. When there is solar thermal energy installed (bs) the biogas production ranges from $0.077m^3/m^3/day$ to $0.088m^3/m^3/day$. This makes an increase of about 14% increases per day when there is a solar thermal energy installed in the bio digester as opposed to when there is no solar thermal energy produced.

From the figure it can be seen that there is heat extraction from the solar storage tank when there is no solar radiation available at night. The circulation pump is continuously pumping heat to the digester. The volume of biogas produced is declining since there is extraction of heat to the digester tank at night when there is no thermal energy supplied

From the graph, it is observed that there is an increase in the volume of biogas produced in the morning at 0080hours to the evening hours at 1700hours when there is solar radiation available and energy is supplied to the solar thermal collectors. Compared to the volume of biogas produced when there is no solar thermal energy installed in the system, there is a significant increase of 14% per day in the volume the biogas produced. The biogas production decreases when there is no solar thermal energy supplied, in this case, heat is extracted from the solar storage tank and supplied to the biodigester. This is a similar case as in figure 19. Heat extracted from the solar storage tanks, decrease the temperature of the collector and the incoming temperature and the collector efficiency decreases.

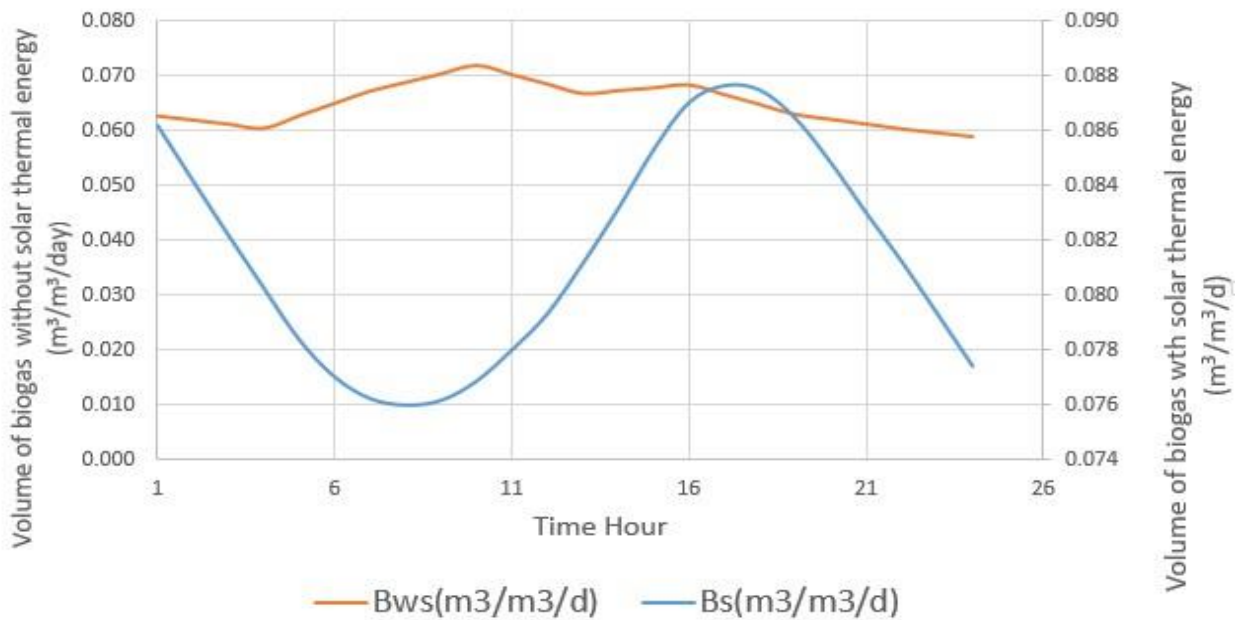


Figure 20: Volume of biogas without solar thermal energy and with solar thermal energy

The prices of energy vary from time to time due to price escalations in the world market[63]. For example, the domestic charge for energy in Lesotho is M1.47/kWh for the year 2020/2021 [64]. This price changes depending on the energy prices in the world market. Using biogas for cooking is like replacing M1.47/kWh of energy used for domestic cooking which acts as the benefit of producing energy from waste since biogas is obtained from waste products. One cubic meter of biogas can do the same work as one cubic meter of liquefied petroleum gases and 1kWh of electrical energy.

Table 3 can be interpreted thus when a collector size of $2m^2$ is used, the biogas produced replaces around 478 $CO_2/kg/year$ of greenhouse gases emitted by wood, 970 $CO_2/kg/year$ of greenhouse gasses emitted by coal, 703 $CO_2/l kg/year$ of kerosene and 534 $CO_2/l kg/year$ of liquefied petroleum gas (LPG). For every collector area deployed there is a volume of biogas produced which replaces certain amount of green house gases that would results from the use of wood,kerosene,LPG and coal.

Table 3: Variation of collector area, the volume of biogas produced and greenhouse gas averted

			Economic Benefits				Environmental Benefits			
Collector (m2)	Bs (m3/yr)	Bws (m3/yr)	Extra biogas (m3/yr.)	Benefits (\$)	Mass biogas (kg)	Price of biofertilizers (kg/\$)	Wood (CO2/kg)	Coal (CO2/kg)	Kerosene (CO2/kg)	LPG (CO2/kg)
2	2749	2504	245	122	281	793	478	970	703	534
3	2772	2504	268	134	308	868	523	1062	769	585
4	2779	2504	275	137	316	890	537	1089	789	600
5	2816	2504	312	156	358	1010	609	1236	896	681
10	2916	2504	412	206	473	1335	805	1633	1183	899
15	3007	2504	503	251	578	1630	983	1994	1445	1098
20	3094	2504	590	295	678	1912	1153	2339	1695	1288
25	3179	2504	675	337	776	2188	1319	2676	1939	1474
30	3262	2504	758	379	871	2457	1481	3006	2178	1655
35	3342	2504	838	419	963	2716	1637	3323	2408	1830
40	3420	2504	916	458	1053	2969	1790	3633	2632	2001
45	3495	2504	991	495	1139	3212	1937	3930	2848	2164
50	3568	2504	1064	532	1223	3449	2079	4220	3058	2324
70	3831	2504	1327	663	1526	4302	2593	5263	3814	2899
80	3940	2504	1436	718	1651	4656	2807	5696	4127	3137

100	4141	2504	1637	818	1882	5307	3200	6493	4705	3576
-----	------	------	------	-----	------	------	------	------	------	------

As outlined by the author in reference [65], biogas results in clean energy which does not cause negative effects on the environment. Figure 19 shows the percentages of greenhouse gases averted per kilogram by biogas production. The use of biogas replaces 18% of CO_2/kg emitted by wood, 26% of CO_2/kg emitted by kerosene, 26% of CO_2/kg emitted by liquefied petroleum gas and 36 % of CO_2/kg emitted coal.

From the pie chart on figure 19, it is apparent that there are greenhouse emissions averted by coal compared to wood, kerosene, and liquefied petroleum gas. The use of biogas replaces greenhouse emissions as compared to other fuels which aims at achieving Sustainable Development Goal seven (SDG7). Another benefit is replacing the use of electricity for cooking and lighting with the use of biogas which can be used for power generation.

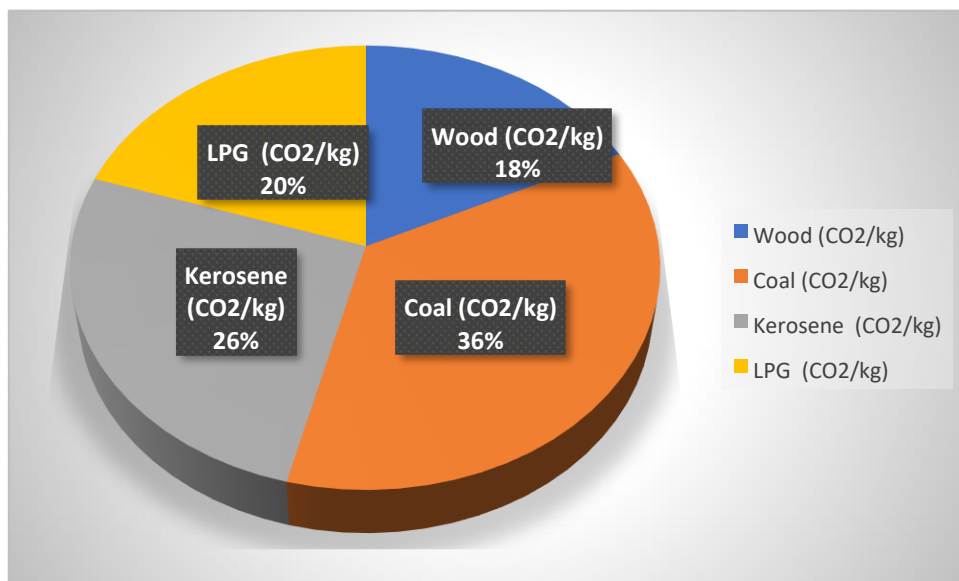


Figure 19: Percentage of greenhouse gases averted

Figure 20 shows the extra benefits of integrating solar thermal collectors to enhance the effectiveness of the biogas production. For different collector areas,

it can be seen that there is an extra benefit of biogas produced and the extra money made in each collector size. Collector area is varied from $2m^2$ up to $100m^2$ observing the extra volume of biogas and the extra money made. For a collector area of $5m^2$, the extra volume of biogas produced is around $312m^3$ per year and the extra money is around \$156 per year. For collector area of $50m^2$, volume biogas produced is around $1064m^3$ per year which is equivalent to the worth \$532 per year.

Conversely as the collector area increases, the marginal increase of the biogas production decreases. There is less extra production of biogas as well as the economic benefits. An optimum collector size is required to obtain an optimum system, since increasing the collector area comes at cost of buying the collectors.

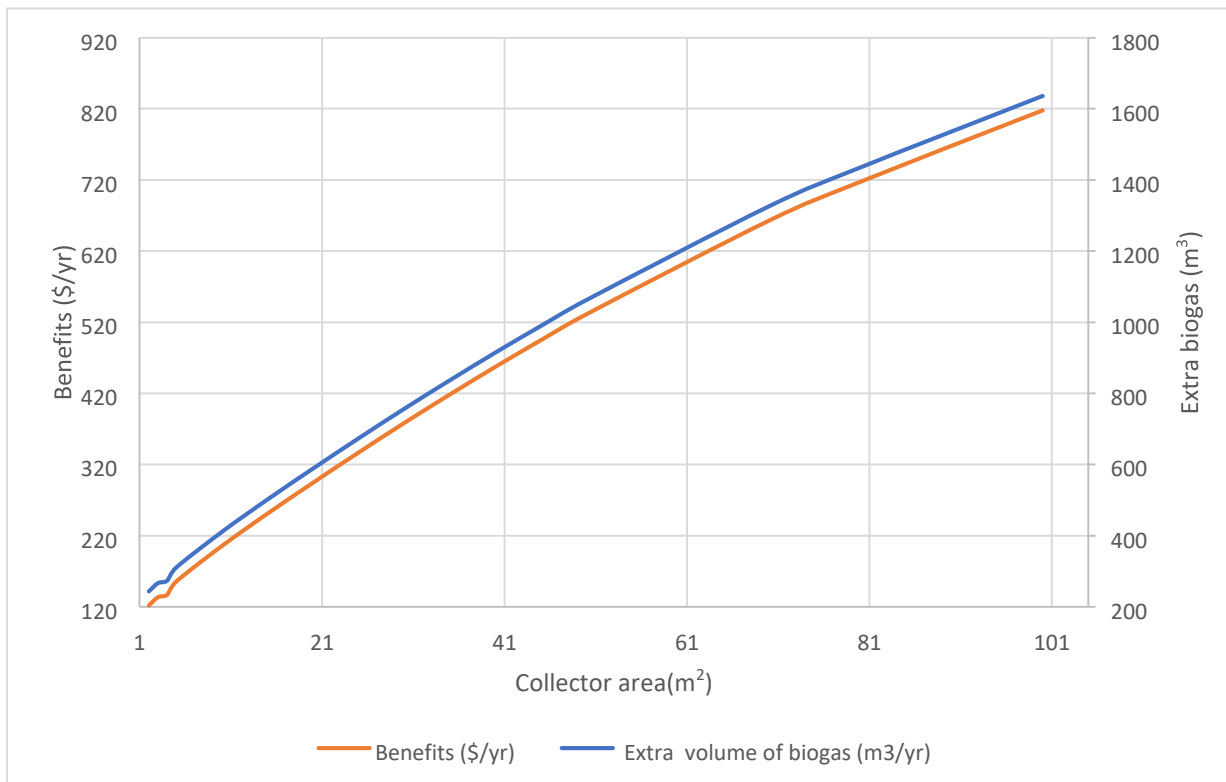


Figure20: Collector area, benefits, and extra biogas production

The production of biogas has some environmental benefits. Biogas production does not only provide a clean form of energy, but it also mitigates greenhouse

gases such as CO₂ emitted by wood, coal, kerosene, Liquid Petroleum Gases. The value of 1m³ biogas is approximately 6 kWh[65], which means more power can be obtained if more biogas is produced. Furthermore 1m³ biogas does the same work as LPG and 1kWh of electricity.

Similarly, figure 21 shows the volume of biogas produced at different collector areas. When the collector area is varied there is an increase in the volume of biogas produced, and the percentage of biogas produced increases as well. However, the graph of collector area against the volume of biogas produced when there is a solar thermal collector installed is not a linear function. The volume of biogas produced increases and then decreases.

As the collector area increases from 2m² to 100m², the volume of biogas with solar thermal energy (bs) increases as well. Nevertheless, the marginal increase of biogas production decreases. That is there is less extra biogas produced as the collector size increases. The economic benefits include the extra volume of biogas and the value of money for the biogas produced at different collector areas. Different collector sizes give different economic benefits and environmental benefits.

From the graph, it could be seen that the marginal increase of biogas production decreases as in domestic solar water heaters. The graphs in figure 22 behave the same way as in figure 20. This means that there is an optimum collector area to deploy to give the architectural design of the system. Increasing the collector area is not always economically viable. There is a need to obtain the optimum collector area.

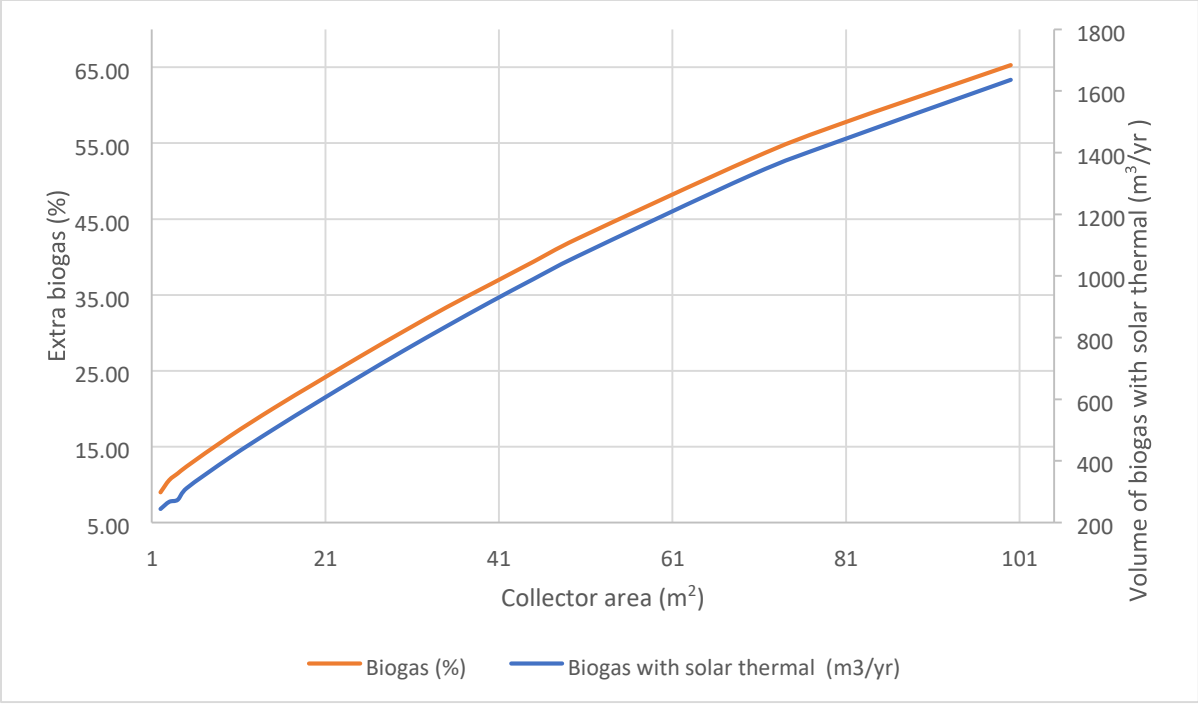


Figure 21: Percentage and volume of biogas produced at different collector areas

4.1 Economic analysis of the system

A successful energy project must have an economic appraisal. In this section, collector costs, storage costs, interest rate, inflation rate, operation and maintenance costs (O&M), Benefit-Cost Ratio, the project payback, Internal Rate of Return as well as Net Present Value are discussed for economic appraisal.

4.1.1 Cash flow analysis

The amount of biogas at each square meter of the collector is multiplied by the price of biogas. In year zero, there are no benefits. In year one, benefits are equal to the difference between the volume of biogas produced when there is no collector compared to the volume of biogas when solar thermal collectors are installed multiplied by the price of one cubic meter of biogas which is found to be \$0.5/m³<https://irena.org/newsroom/articles/2017/Mar/Biogas-CostReductions-to-Boost-Sustainable-Transport>. The benefits is the number of extra cubic meter of biogas produced multiplied by the price of one cubic meter biogas.

System cost is the collector area multiplied by the cost per square meter of the collector. Benefits are likely to change due to price escalation. The price escalation is due to the rise in energy prices in the market. However, for the rest of the years, the cost is just operations and maintenance. Net cash flow is the difference between cost and benefits.

4.1.2 System optimization

The name of collector chosen for system design is the sun power (ETC) with the optimum collector area of 16m². The energy per dollar is 25.3 kWh and cost of sun power evacuated tube collector is \$59/m² which makes a total cost of buying the collectors be \$944. When an optimum collector area of 16m² is used the

storage volume is around 880 liters. However, it is not practical to have a solar storage volume of 880 liters. Since the solar storage tanks are sold multiples of 100litres or multiples of 50litres.

It is observed that when 800litres of the solar storage tank is used. The maximum NPV of \$1854 is found. However other storage volumes 900litres and 1000Litres of solar storage solar tank give minimum NPV compared to 800 liters. The extra biogas produced is around $396m^3$ per annum. The biodigester produces more biogas at the mesophilic temperature range of $18^{\circ}C$ to $30^{\circ}C$.

When the collector area is $16m^2$, the solar storage tank of 800 liters and the digester tank of 5000litres are found. The system gives optimum results. The total benefit is \$4806, a total cost of \$ 1889 including operation and maintenance (O & M).

Table 4 shows the project cash flow analysis for a lifetime of 20 years. From the table, it is observed that the benefits and net cash flow are increasing from year 1 to year 20. While on the other hand, the Present Value (PV) and the discount factor is decreasing over the year. However, before the end of the first year of investment, the total cost is the cost of buying the collector and the cost of storage. For the project lifetime of 20 years, the net cash flow is \$ 2917 and the Net Present Value is \$1854.

Both the present benefits and the present cost are decreasing over a period of twenty years. This is because the present benefits and the present costs are calculated using the discount factor. The Present Value of benefits is \$3673 and the Present Value costs is \$ 1819. The Benefit Cost Ratio is 2.01 for a period of twenty years .

Table 4: Cash flow analysis for the project lifetime

Price Escalation	year 1	Benefits	PV Benefits	Cost(\$)	PV Costs	Net Cash Flow	Discount Factor	PV	Cum.PV/m ³
2%	0	0	0	1574	1574	-1574	1.0000	-1574	-1574
O&M Cost	1	198	193	16	15	182	0.9753	178	-1397
1%	2	202	192	16	15	186	0.9512	177	-1220
Discount rate	3	206	191	16	15	190	0.9276	176	-1043
2.536%	4	210	190	16	14	194	0.9047	176	-868
inflation	5	214	189	16	14	198	0.8823	175	-693
4.90%	6	218	188	16	14	203	0.8605	174	-518
interest Rate	7	223	187	16	13	207	0.8392	174	-344
7.56%	8	227	186	16	13	211	0.8185	173	-171
	9	232	185	16	13	216	0.7982	172	1
	10	236	184	16	12	221	0.7785	172	173
	11	241	183	16	12	225	0.7592	171	344
	12	246	182	16	12	230	0.7405	170	514
	13	251	181	16	11	235	0.7221	170	684
	14	256	180	16	11	240	0.7043	169	853
	15	261	179	16	11	245	0.6869	168	1022
	16	266	178	16	11	250	0.6699	168	1190
	17	272	177	16	10	256	0.6533	167	1357
	18	277	176	16	10	261	0.6372	166	1523
	19	283	176	16	10	267	0.6214	166	1689
	20	288	175	16	10	272	0.6060	165	1854
Total		4806	3673	1889	1819	2917		1854	

Benefit CostRatio(BCR)	2.019496								
-------------------------------	-----------------	--	--	--	--	--	--	--	--

4.1.3 Project Payback Period

The payback period has been analyzed to check the economic viability of the project. Figure 22 shows the project payback period with a project lifetime of 20 years. From the figure, it can be seen that the Net Present Value is negative in the initial investment period. The graph shows that NPV increases from the negative NPV initial year of investment until it reaches zero. In this case, the project is not economically viable since the Net Present Value is negative, but it becomes economically viable when the Net Present Value is positive.

A shorter payback period is recommended for the lifetime investment of the energy project. From the graph, the project payback is around eight years which is less than the project lifetime. This is a shorter payback period which makes the project economically viable.

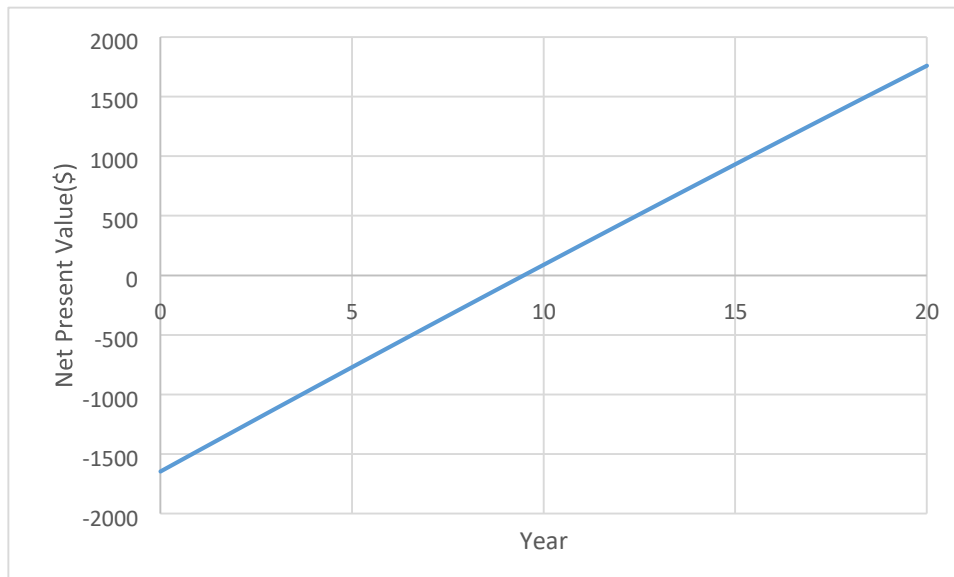


Figure 22: : Payback Period

4.1.4 Net Present Value

Similar to the project Payback Period, the Net Present Value also depends on the prevailing interest rate and the inflation rates. Illustrated in figure 23 is a graph that shows how the Net Present Value changes as the collector area increases. From the graph, it can be seen that the graph is not a linear function. The Net Present Value increases then decreases as the collector area increases until Net Present Value reaches zero. As the collector area increases the Net Present Value increases and then decreases until it reaches zero and then becomes negative.

The design locus is found at the elbow. The optimum collector area lies below $20m^2$. The optimum collector area which gives the highest Net Present Value is around $16m^2$ with a Net Present Value of \$1854. The project is viable for a small collector area. If the collector area increases more, the Net Present Value decreases.

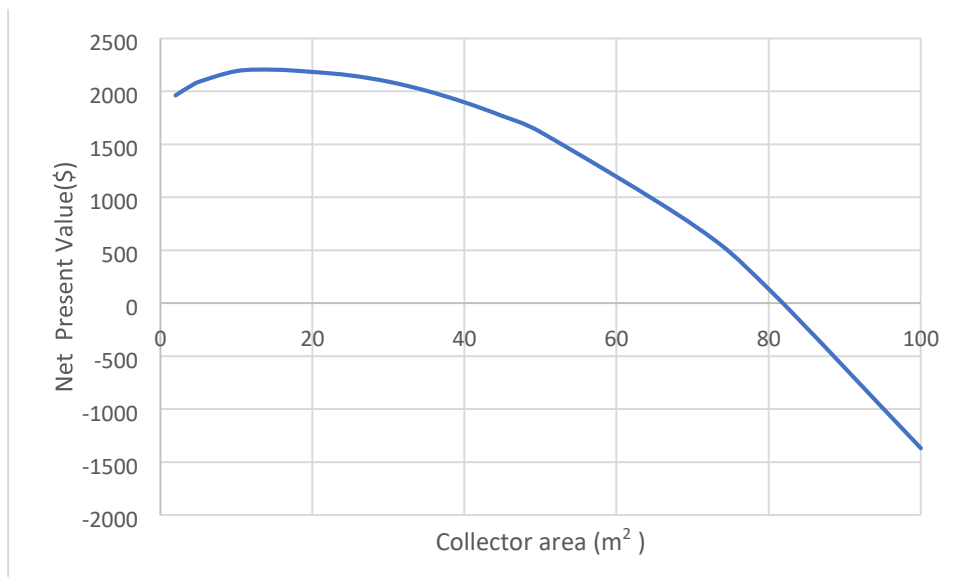


Figure 23: Collector area against Net Present Value

4.1.4 Internal Rate of Return

As discussed in section two, another economic indicator that measures the project's wealth is the Internal Rate of Return. Internal Rate of Return is the value of discount rate in which the Net Present Value is equal to zero. Figure 24 shows how the discount rate varies against Net Present Value. The graph of discount rate against the Net Present Value is not a linear function. From the graph, it can be observed that the Net Present Value decreases (NPV) as the discount rate increases until NPV is equal to zero.

The discount rate is the rate at which an investor is expected to get at the end of the investment period. From figure 24 internal rate of return is about 10.36%, which means beyond 10.36% the project is not viable since the Net Present Value is negative. At 10.36%, the Net Present Value of the cost (negative cash flow) is equal to the Net Present Value of the benefits (positive cash flow). The value of the Internal Rate of Return is high. In terms of project IRR, the project is also found to be economically viable since project IRR is greater than the interest rate.

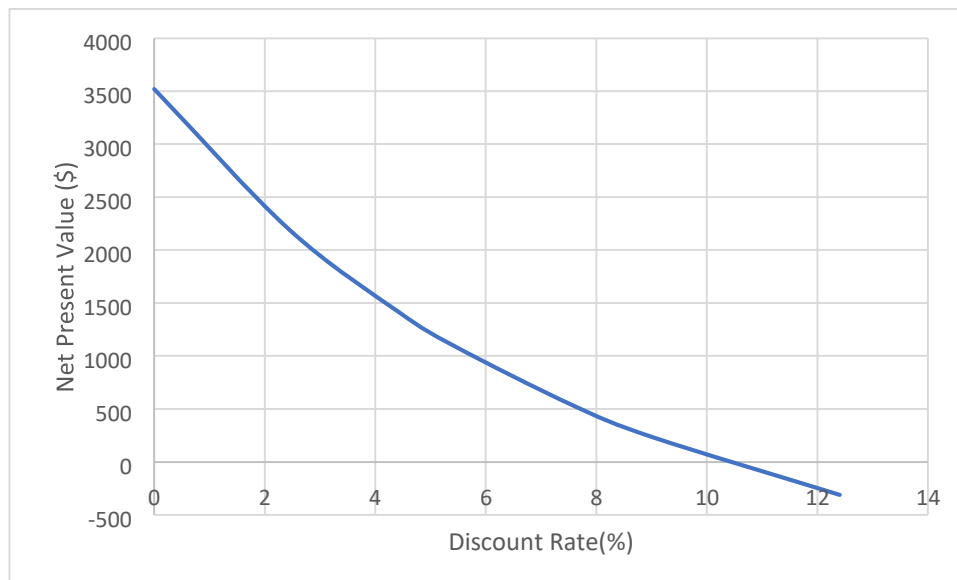


Figure 24: Internal Rate of Return

Table 5 shows the economic assessment for the project. The economic performance indicators which measure the project performances are discussed. The project viability has been assessed using the prevailing profitability index of inflation of 4.9%, and an interest rate of 7.56%. The project lifetime is twenty years with, a discount rate of 2.53 %, a Cost-Benefit Ratio of 2.01, an internal rate of return of 10.35%, a maximum NPV is \$1854, and a payback period of 9 years. The project is found to be economically viable since the project IRR is greater than the interest rate.

Table 5:Results for economic assessment of an integrated solar assisted solar biogas

Profitability index $i=7.56\%$, $j=4.9\%$, $r = 2.53\%$, $n=20$	Financial assessment
Net Present Value (NPV)(\$)	1854
Internal Rate of Return (IRR) (%)	10.35
Project payback Period(years)	9
Benefit-Cost Ratio	2.01

4.1.5 Validation of results

The study has been analyzed using the Payback period, Net Present Value, Cost Benefit Ratio and Internal Rate of Return to find the economic viability of solar thermal energy. As discussed in the literature, some studies have been done to check the economic viability of energy projects using economic performance indicators.

The discussed studies in the literature found out that a payback period ranges from 3 years to 11 years, even though this differs from project to project depending on the size of the plant. The Net Present Value has also been found

positive and the Internal Rate of Return is high compared to the interest rate. The research project is found to be economically viable since the NPV, Payback Period and Internal Rate of Return are within the range of the previous study in the literature.

4.1.6 Limitations of the study

The research has been carried out using TMY data. It has been said in the literature that TMY data found from PVGIS is less accurate compared to National Aeronautics and Space Administration (NASA) data. While on the other hand, the NASA data is not always available. The use of TMY data from PVGIS makes the results not accurate due to lack of accuracy found in the data. On the other hand, the computation of incident angle modifier ($K_{\tau\alpha}$) has been omitted when calculating the efficiency of the collector (η_{col}) due to lack of time, since it is tedious and cumbersome. This also makes the results less accurate compared to when the incident angle modifier has been included in the calculation.

In this section the clear synthesis of the results linking with the objectives and the literature was discussed. Tables and graphs which gave an idea of major findings were discussed.

In the next section, conclusion will be drawn from major findings and policy recommendations will be discussed. Based on the major findings policy recommendations will be taken into consideration in order to advice policy makers.

5.0. Conclusion and recommendations

The study presented an optimally integrated solar thermal model to enhance biogas production. The optimal size of the solar storage tank collector area has been found. Both economic and thermal analyses of the system have been found. Using the excel-based model the system with geometric data inputs, thermal inputs, and economic inputs. The simulations have been performed in an hourly time step.

Sun power evacuated tube collector is the best collector due to its low cost in the market with the solar thermal collector optical efficiency of 0.412 ($F_{RT}\alpha$) and heat loss parameter (F_{RUL}) of 1.501. The collector warranty is 5 years. It was found that when the solar thermal energy is installed in the biodigester, the biogas production rate increases. The biogas production rate is 396 m^3 per annum for a 5 m^3 digester. The rate of biogas production is high at a mesophilic temperature between 18⁰ C to 30⁰ C. The correlation equation between the digester temperature and volume of biogas produced is found to be $V_{biogas} = -0.001 T_d^2 + 0.0164 T_d + 0.0399$.

It was also found out that for 5 m^3 biodigester, the optimum collector area (A_c) is 16 m^2 and a solar storage tank of 800 liters is required. Furthermore 1 m^3 of biodigester requires a collector area of about 3 m^2 . The total cost of buying the collector and the solar storage tank is \$1744. The optimum collector area gives a maximum Net Present Value of \$1854. Moreover, the extra biogas produced is 396 m^3 per annum with the percentage increase of extra biogas as 11.5% per annum. The project is found to be economically viable with a Net Present Value of \$1854, an Internal Rate of Return of 10.36%, a Payback period of 8 years, and a Benefit-Cost Ratio of 2.01, and a discount rate of 2.53%.

Several people can benefit from the study. Investors, NGOs, individuals, and policymakers can benefit from the research study. The research study helps the

investors in investment making decisions whether to go for the project or not. The latter will benefit by making clear policy guidelines with the intended outcomes for bioenergy technology. Therefore, there is a need for energy policymakers to promote the use of bioenergy and shift from the traditional use of biomass to the modern use of biomass.

The Lesotho energy policy 2015 has only one policy statement (energy policy statement 3), which talks about the use of bioenergy. The rest of the fourteen policy statements talk about other renewable technologies. The production of biogas using solar thermal technology does not only provide economic benefits, reduces the carbon dioxide produced.

6.0 References

- [1] K. K. Gopinathan, "Solar energy utilization in Lesotho." 1989.
- [2] A. Nelabhotla and C. Dinamarca, "Bioelectrochemical CO₂ Reduction to Methane: MES Integration in Biogas Production Processes," *Appl. Sci.*, vol. 9, no. 6, p. 1056, Mar. 2019, doi: 10.3390/app9061056.
- [3] M. D. Ghatak and P. Mahanta, "Effect of Temperature on Anaerobic Co-digestion of Cattle dung with Lignocellulosic Biomass," p. 7, 2014.
- [4] J. Ajayan, D. Nirmal, P. Mohankumar, M. Saravanan, M. Jagadesh, and L. Arivazhagan, "A review of photovoltaic performance of organic/inorganic solar cells for future renewable and sustainable energy technologies," *Superlattices Microstruct.*, vol. 143, p. 106549, Jul. 2020, doi: 10.1016/j.spmi.2020.106549.
- [5] B. M. Taele, K. K. Gopinathan, and L. Mokhuts'oane, "The potential of renewable energy technologies for rural development in Lesotho," *Renew. Energy*, vol. 32, no. 4, pp. 609–622, Apr. 2007, doi: 10.1016/j.renene.2006.02.014.
- [6] E. S. Gaballah, T. K. Abdelkader, S. Luo, Q. Yuan, and A. El-Fatah Abomohra, "Enhancement of biogas production by integrated solar heating system: A pilot study using tubular digester," *Energy*, vol. 193, p. 116758, Feb. 2020, doi: 10.1016/j.energy.2019.116758.
- [7] F. B. Agyenim, "Powering communities using hybrid solar--biogas in Ghana, a feasibility study," *Environ. Technol.*, p. 11, 2020.
- [8] S. Wang, F. Ma, W. Ma, P. Wang, G. Zhao, and X. Lu, "Influence of Temperature on Biogas Production Efficiency and Microbial Community in a Two-Phase Anaerobic Digestion System," *Water*, vol. 11, no. 1, p. 133, Jan. 2019, doi: 10.3390/w11010133.
- [9] S. Wang, F. Ma, W. Ma, P. Wang, G. Zhao, and X. Lu, "Influence of Temperature on Biogas Production Efficiency and Microbial Community in a Two-Phase Anaerobic Digestion System," *Water*, vol. 11, no. 1, p. 133, Jan. 2019, doi: 10.3390/w11010133.
- [10] T. Hove, "A Thermo-Economic Model for Aiding Solar Collector Choice and Optimal Sizing for a Solar Water Heating System," in *Africa-EU Renewable Energy Research and Innovation Symposium 2018 (RERIS 2018)*, M. Mpholo, D. Steuerwald, and T. Kukeera, Eds. Cham: Springer International Publishing, 2018, pp. 1–19.
- [11] L. Lombardi, B. Mendecka, and S. Fabrizi, "Solar Integrated Anaerobic Digester: Energy Savings and Economics," *Energies*, vol. 13, no. 17, p. 4292, Aug. 2020, doi: 10.3390/en13174292.
- [12] A. Faaij, "Modern Biomass Conversion Technologies," *Mitig. Adapt. Strateg. Glob. Change*, vol. 11, no. 2, pp. 343–375, Mar. 2006, doi: 10.1007/s11027-005-9004-7.
- [13] Kumar et al., "A review on biomass energy resources, potential, conversion and policy in India." 2014.
- [14] H. M. Mahmudul, M. G. Rasul, D. Akbar, R. Narayanan, and M. Mofijur, "A comprehensive review of the recent development and challenges of a solar-assisted biodigester system," *Sci. Total Environ.*, vol. 753, p. 141920, Jan. 2021, doi: 10.1016/j.scitotenv.2020.141920.

- [15] X. Fei *et al.*, “Enhancement effect of ionizing radiation pretreatment on biogas production from anaerobic fermentation of food waste,” *Radiat. Phys. Chem.*, vol. 168, p. 108534, Mar. 2020, doi: 10.1016/j.radphyschem.2019.108534.
- [16] T. W. M. Amen, O. Eljamal, A. M. E. Khalil, and N. Matsunaga, “Evaluation of sulfatecontaining sludge stabilization and the alleviation of methanogenesis inhibition at mesophilic temperature,” *J. Water Process Eng.*, vol. 25, pp. 212–221, Oct. 2018, doi: 10.1016/j.jwpe.2018.08.004.
- [17] Y. Zhong *et al.*, “Using anaerobic digestion of organic wastes to biochemically store solar thermal energy,” *Energy*, vol. 83, pp. 638–646, Apr. 2015, doi: 10.1016/j.energy.2015.02.070.
- [18] P. Guo, J. Zhou, R. Ma, N. Yu, and Y. Yuan, “Biogas Production and Heat Transfer Performance of a Multiphase Flow Digester,” *Energies*, vol. 12, no. 10, p. 1960, May 2019, doi: 10.3390/en12101960.
- [19] B. Ouhammou, M. Aggour, Â. Frimane, M. Bakraoui, H. El Bari, and A. Essamri, “A new system design and analysis of a solar bio-digester unit,” *Energy Convers. Manag.*, vol. 198, p. 111779, Oct. 2019, doi: 10.1016/j.enconman.2019.111779.
- [20] S. Gorjian, H. Ebadi, F. Calise, A. Shukla, and C. Ingraio, “A review on recent advancements in performance enhancement techniques for low-temperature solar collectors,” *Energy Convers. Manag.*, vol. 222, p. 113246, Oct. 2020, doi: 10.1016/j.enconman.2020.113246.
- [21] Y. Tian and C. Y. Zhao, “A review of solar collectors and thermal energy storage in solar thermal applications,” *Appl. Energy*, vol. 104, pp. 538–553, Apr. 2013, doi: 10.1016/j.apenergy.2012.11.051.
- [22] S. A. Kalogirou, “Use of TRNSYS for modelling and simulation of a hybrid pv–thermal solar system for Cyprus,” *Renew. Energy*, vol. 23, no. 2, pp. 247–260, Jun. 2001, doi: 10.1016/S0960-1481(00)00176-2.
- [23] S. K. Chaturvedi and M. Abazeri, “Transient simulation of a capacity-modulated, directexpansion, solar-assisted heat pump,” *Sol. Energy*, vol. 39, no. 5, pp. 421–428, 1987, doi: 10.1016/S0038-092X(87)80060-9.
- [24] M. Kao, “OPTIMIZATION OF THE CHOICE OF SOLAR MINIGRID ARCHITECTURE AND MANAGEMENT IN LESOTHO,” 2020.
- [25] T. M. Klucher, “Evaluation of models to predict insolation on tilted surfaces,” *Sol. Energy*, vol. 23, no. 2, pp. 111–114, 1979, doi: 10.1016/0038-092X(79)90110-5.
- [26] E. G. Evseev and A. I. Kudish, “The assessment of different models to predict the global solar radiation on a surface tilted to the south,” *Sol. Energy*, vol. 83, no. 3, pp. 377–388, Mar. 2009, doi: 10.1016/j.solener.2008.08.010.
- [27] A. Rabl, “THE AVERAGE DISTRIBUTION OF SOLAR RADIATION--CORRELATIONS BETWEEN DIFFUSE AND HEMISPHERICAL AND BETWEEN DAILY AND HOURLY INSOLATION VALUES,” p. 10.
- [28] J. A. Duffie and W. A. Beckman, “Solar Engineering of Thermal Processes,” p. 928.
- [29] A. Q. Jakhriani, S. R. Samo, A. R. H. Rigit, and S. A. Kamboh, “Selection of Models for Calculation of Incident Solar Radiation on Tilted Surfaces,” p. 10, 2013.

- [30] Kumar Pandey Chanchal and A. K. Katiyar, “A note on diffuse solar radiation on a tilted surface.” Jul. 2009.
- [31] J. A. Duffie and W. A. Beckman, “Solar Engineering of Thermal Processes,” p. 928. [32] S. Kalogirou, *Solar energy engineering: processes and systems*, Second edition. Amsterdam ; Boston: Elsevier, AP, Academic Press is an imprint of Elsevier, 2014.
- [33] M. R. Kumar, B. B. S. Babu, and M. Seshu, “Estimation of Average Solar Radiation on Horizontal and Tilted Surfaces for Vijayawada Location,” p. 11.
- [34] J. A. Duffie and W. A. Beckman, “Solar Engineering of Thermal Processes,” p. 928.
- [35] T. Hove, “Energy delivery of solar thermal collectors in Zimbabwe,” 2000.
- [36] G. N. Kulkarni, S. B. Kedare, and S. Bandyopadhyay, “Design of solar thermal systems utilizing pressurized hot water storage for industrial applications,” *Sol. Energy*, vol. 82, no. 8, pp. 686–699, Aug. 2008, doi: 10.1016/j.solener.2008.02.011.
- [37] A. Gautam, S. Chamoli, A. Kumar, and S. Singh, “A review on technical improvements, economic feasibility and world scenario of solar water heating system,” *Renew. Sustain. Energy Rev.*, vol. 68, pp. 541–562, Feb. 2017, doi: 10.1016/j.rser.2016.09.104.
- [38] S. Dhanushkodi, V. H. Wilson, and K. Sudhakar, “Life Cycle Cost of Solar Biomass Hybrid Dryer Systems for Cashew Drying of Nuts in India,” *Environ. Clim. Technol.*, vol. 15, no. 1, pp. 22–33, Dec. 2015, doi: 10.1515/rtuct-2015-0003.
- [39] O. Žižlavský, “Net Present Value Approach: Method for Economic Assessment of Innovation Projects,” *Procedia - Soc. Behav. Sci.*, vol. 156, pp. 506–512, Nov. 2014, doi: 10.1016/j.sbspro.2014.11.230.
- [40] A. Barragán-Escandón, J. M. Olmedo Ruiz, J. D. Curillo Tigre, and E. F. Zalamea-León, “Assessment of Power Generation Using Biogas from Landfills in an Equatorial Tropical Context,” *Sustainability*, vol. 12, no. 7, p. 2669, Mar. 2020, doi: 10.3390/su12072669. [41] S. C. Bhattacharyya, *Energy Economics*. London: Springer London, 2011.
- [42] A. S. O. Ogunjuyigbe, T. R. Ayodele, and M. A. Alao, “Electricity generation from municipal solid waste in some selected cities of Nigeria: An assessment of feasibility, potential and technologies,” *Renew. Sustain. Energy Rev.*, vol. 80, pp. 149–162, Dec. 2017, doi: 10.1016/j.rser.2017.05.177.
- [43] M. EL-Shimy, “Analysis of Levelized Cost of Energy (LCOE) and grid parity for utilityscale photovoltaic generation systems,” 2012, doi: 10.13140/RG.2.2.10311.29603.
- [44] R. S. Ali, “BIOGAS PRODUCTION FROM POULTRY MANURE USING A NOVEL SOLAR ASSISTED SYSTEM,” p. 105, 2015.
- [45] O. Adeoti, M. O. Ilori, T. O. Oyebisi, and L. O. Adekoya, “Engineering design and economic evaluation of a family-sized biogas project in Nigeria,” *Technovation*, vol. 20, no. 2, pp. 103–108, Feb. 2000, doi: 10.1016/S0166-4972(99)00105-4.
- [46] R. S. Ali, “BIOGAS PRODUCTION FROM POULTRY MANURE USING A NOVEL SOLAR ASSISTED SYSTEM,” p. 105, 2015.
- [47] S. Yuan, T. Rui, and Y. X. Hong, “Research and Analysis of Solar Heating Biogas Fermentation System,” *Procedia Environ. Sci.*, vol. 11, pp. 1386–1391, 2011, doi: 10.1016/j.proenv.2011.12.208.
- [48] E. S. Gaballah, T. K. Abdelkader, S. Luo, Q. Yuan, and A. El-Fatah Abomohra,

- “Enhancement of biogas production by integrated solar heating system: A pilot study using tubular digester,” *Energy*, vol. 193, p. 116758, Feb. 2020, doi: 10.1016/j.energy.2019.116758.
- [49] L. Lombardi, B. Mendecka, and S. Fabrizi, “Solar Integrated Anaerobic Digester: Energy Savings and Economics,” *Energies*, vol. 13, no. 17, p. 4292, Aug. 2020, doi: 10.3390/en13174292.
- [50] N. Curry and P. Pillay, “Integrating solar energy into an urban small-scale anaerobic digester for improved performance,” *Renew. Energy*, vol. 83, pp. 280–293, Nov. 2015, doi: 10.1016/j.renene.2015.03.073.
- [51] D. Borello, “Modelling of a CHP SOFC system fed with biogas from anaerobic digestion of municipal waste integrated with solar collectors and storage unit,” *Int. J. Thermodyn.*, vol. 16, no. 1, pp. 28–35, Dec. 2012, doi: 10.5541/ijot.451.
- [52] G. Merlin, F. Kohler, M. Bouvier, T. Lissolo, and H. Boileau, “Importance of heat transfer in an anaerobic digestion plant in a continental climate context,” *Bioresour. Technol.*, vol. 124, pp. 59–67, Nov. 2012, doi: 10.1016/j.biortech.2012.08.018.
- [53] J. Martí-Herrero, R. Alvarez, and T. Flores, “Evaluation of the low technology tubular digesters in the production of biogas from slaughterhouse wastewater treatment,” *J. Clean. Prod.*, vol. 199, pp. 633–642, Oct. 2018, doi: 10.1016/j.jclepro.2018.07.148.
- [54] H. M. Mahmudul, M. G. Rasul, D. Akbar, and M. Mofijur, “Opportunities for solar assisted biogas plant in subtropical climate in Australia: A review,” *Energy Procedia*, vol. 160, pp. 683–690, Feb. 2019, doi: 10.1016/j.egypro.2019.02.192.
- [55] M. Mohammed *et al.*, “Feasibility study for biogas integration into waste treatment plants in Ghana,” *Egypt. J. Pet.*, vol. 26, no. 3, pp. 695–703, Sep. 2017, doi: 10.1016/j.ejpe.2016.10.004.
- [56] S. Achinas and G. Euverink, “Feasibility Study of Biogas Production from Hardly Degradable Material in Co-Inoculated Bioreactor,” *Energies*, vol. 12, no. 6, p. 1040, Mar. 2019, doi: 10.3390/en12061040.
- [57] A. K. Singh, S. Poonia, D. Jain, D. Mishra, and R. K. Singh, “Economic evaluation of a business model of selected solar thermal devices in Thar Desert of Rajasthan, India,” vol. 22, no. 3, p. 9, 2020.
- [58] G. Vijayakumar, “ASSESSMENT OF SOLAR RADIATION DATA USED IN ANALYSES OF SOLAR ENERGY SYSTEMS,” p. 101.
- [59] Ludwig Sasse, “Sasse biogas plants,” 1988.
- [60] P. J. Jørgensen, “Biogas - green energy,” 2009.
- [61] Terrence J. Toy, “The prediction of mean monthly soil temperature from mean monthly air temperature,” 1978.
- [62] H. Binici, O. Aksogan, M. N. Bodur, E. Akca, and S. Kapur, “Thermal isolation and mechanical properties of fibre reinforced mud bricks as wall materials,” *Constr. Build. Mater.*, vol. 21, no. 4, pp. 901–906, Apr. 2007, doi: 10.1016/j.conbuildmat.2005.11.004.
- [63] G. R. Dahal, “COST-BENEFIT ANALYSIS OF REPLACING LPG STOVES WITH INDUCTION STOVES IN RURAL HOUSEHOLDS OF KAVRE DISTRICT, NEPAL,” p. 119.
- [64] LEWA, “Lesotho Electricity and Water Authority report,” 2020 2021.

[65] R. Agrahari and G. N. Tiwari, "The Production of Biogas Using Kitchen Waste," *Int. J. Energy Sci.*, vol. 3, no. 6, p. 408, 2013, doi: 10.14355/ijes.2013.0306.05.

